



A.D. 1308
unipg
DIPARTIMENTO
DI FISICA E GEOLOGIA

ECT*

EUROPEAN CENTRE FOR THEORETICAL STUDIES
IN NUCLEAR PHYSICS AND RELATED AREAS



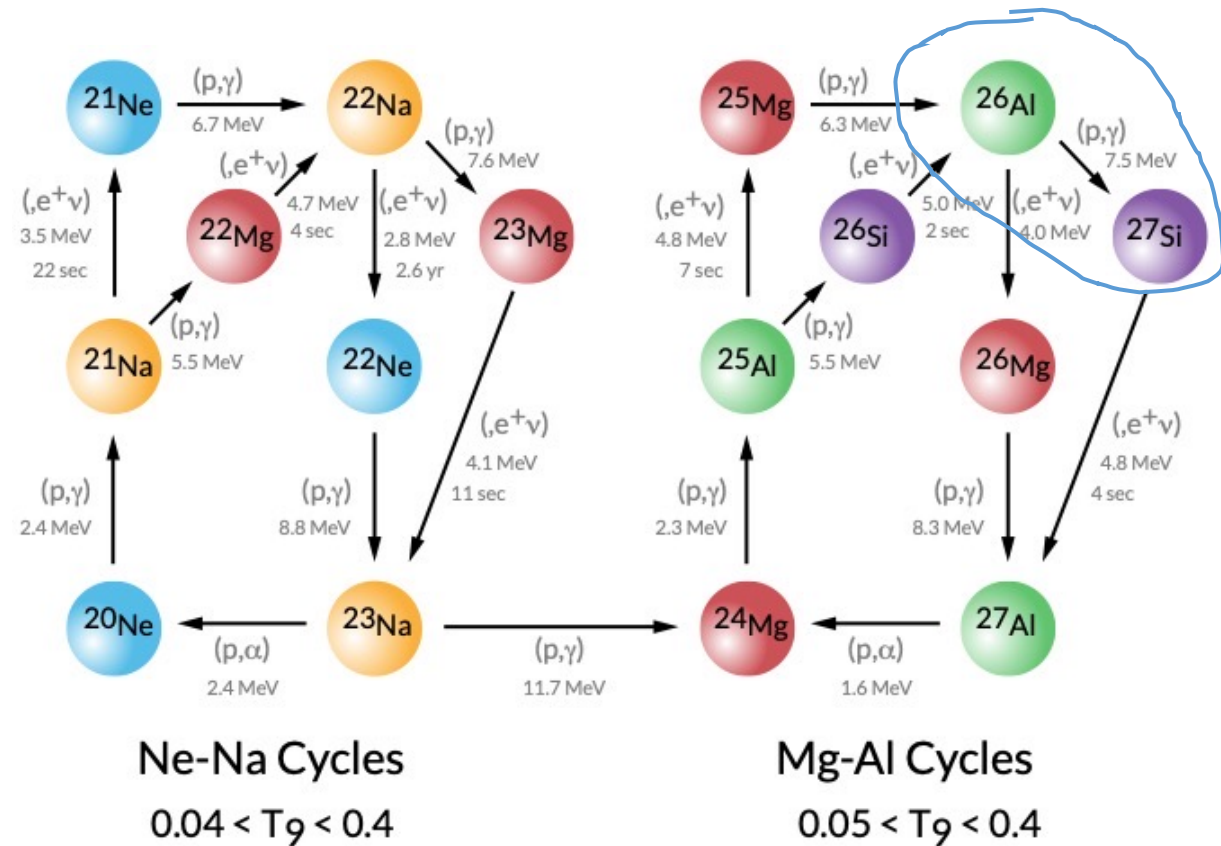
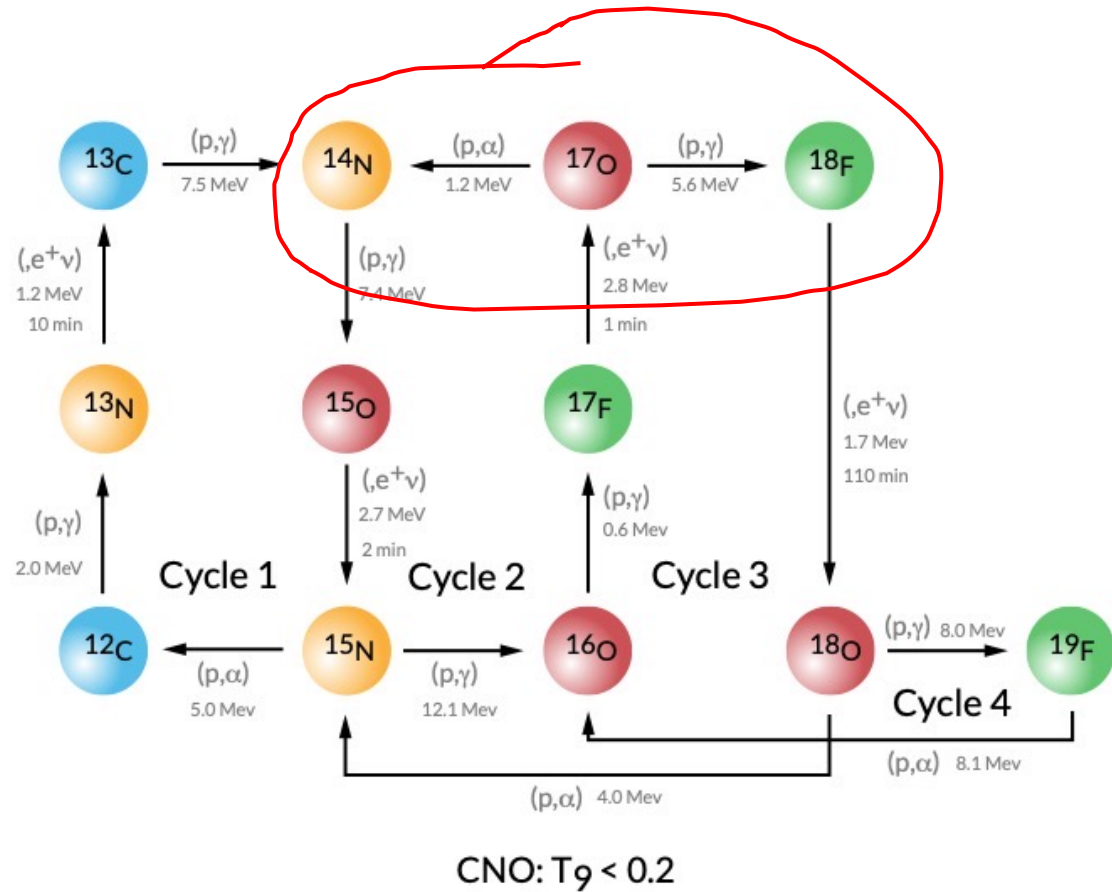
KEY REACTIONS IN NUCLEAR ASTROPHYSICS

$^{17}\text{O}+p$ & $^{26}\text{Al}+p$ REACTION RATES, H-BURNING AND STELLAR MASSES

SARA PALMERINI

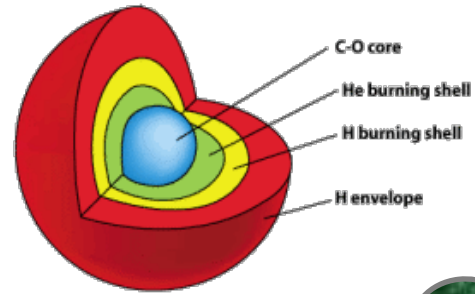
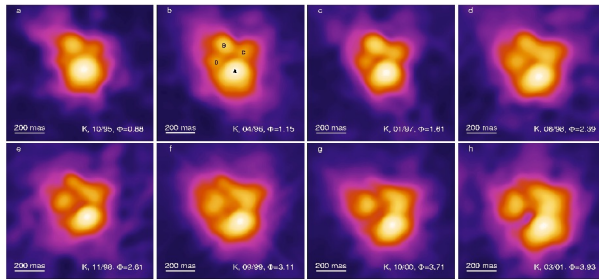
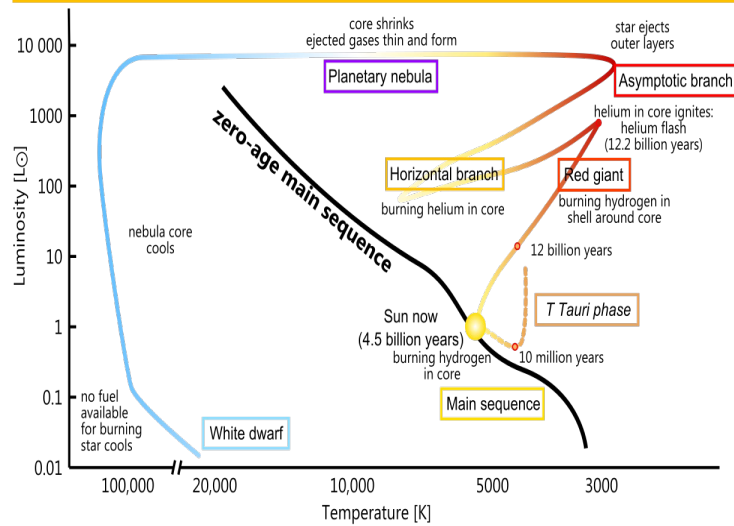
UNIVERSITA' DEGLI STUDI DI PERUGIA & INFN SEZ. PERUGIA, ITALY

$^{17}\text{O} + p$ & $^{26}\text{Al} + p$ REACTIONS IN H-BURNING

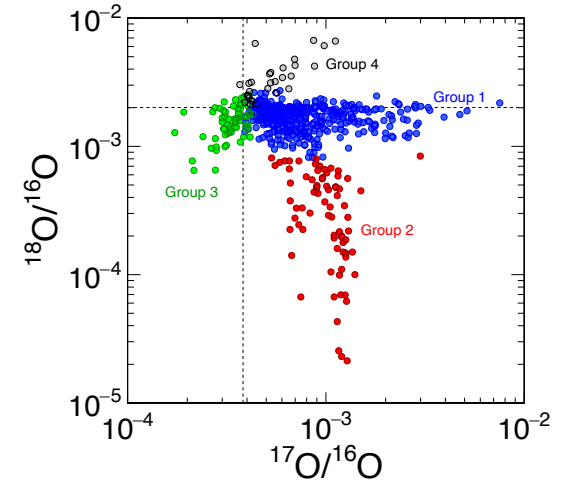
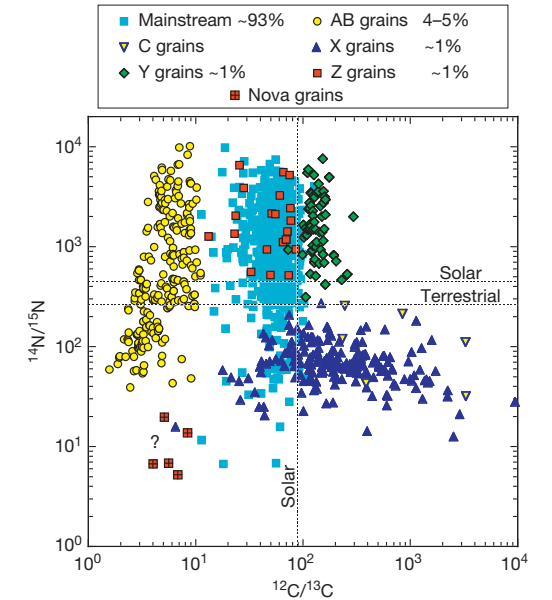
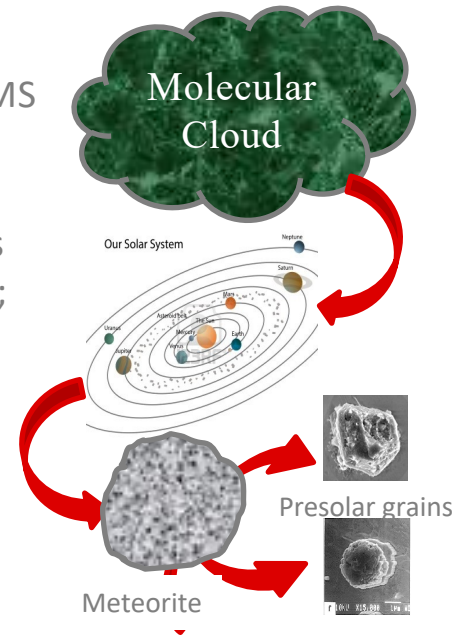


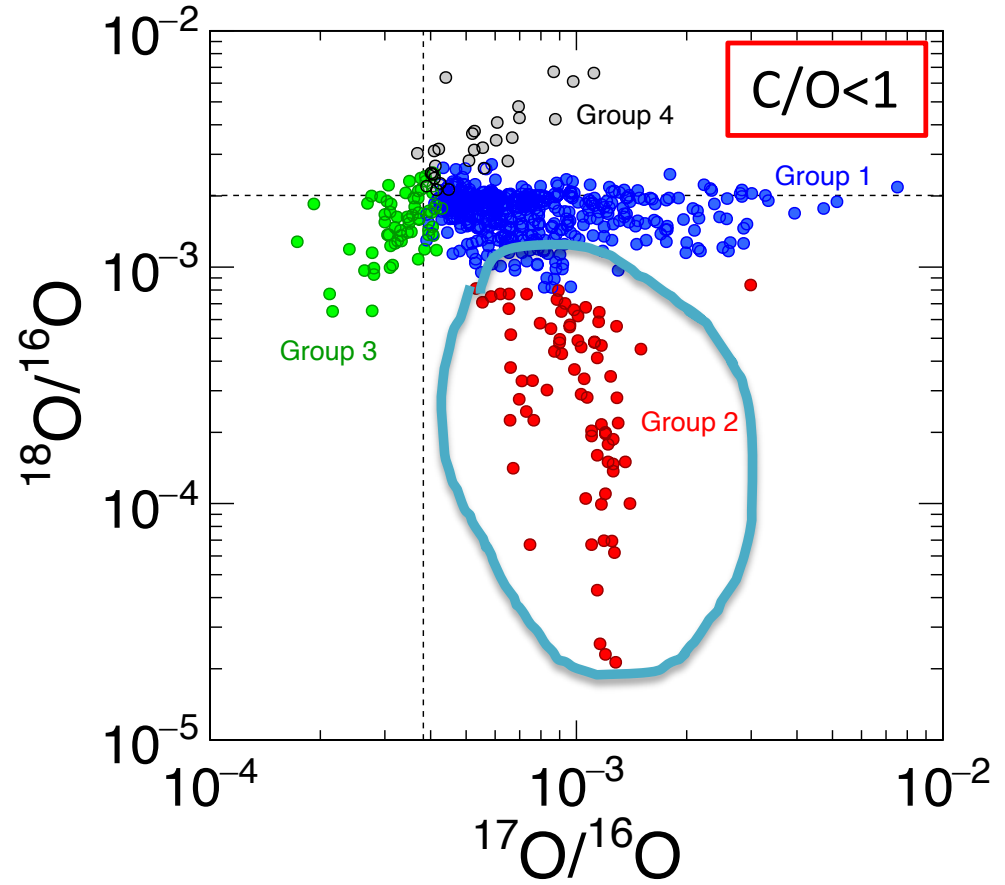
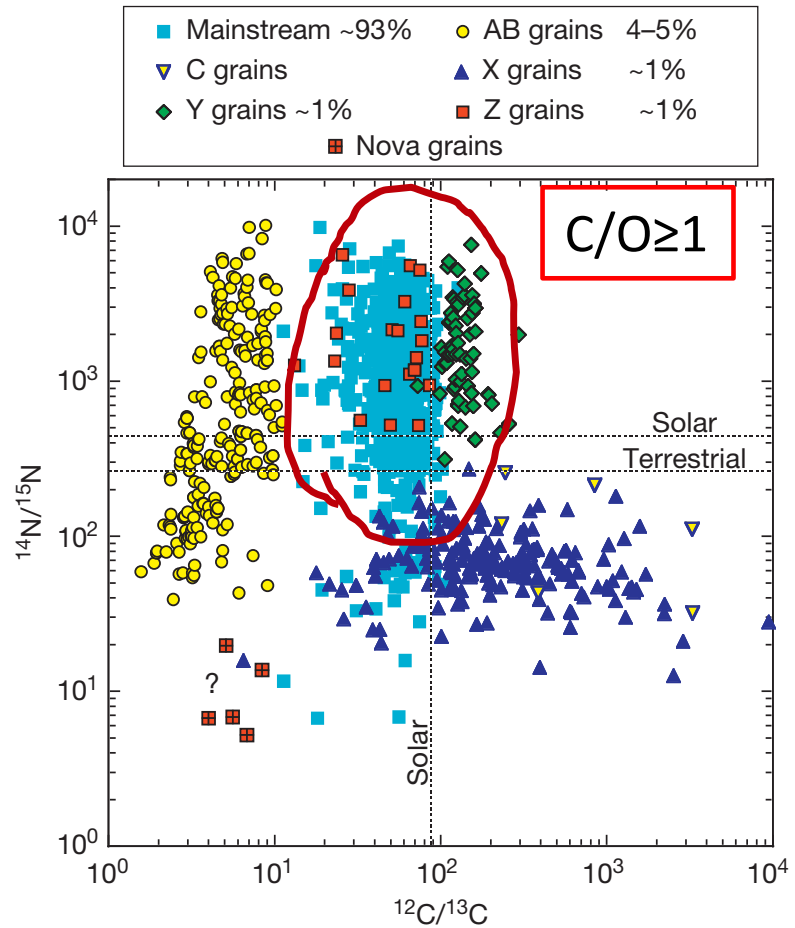
AGB STARS: A VERY BRIEF INTRODUCTION

Stage:	~9 Ga	~1 Ga	~100 Ma	~10 000 a	
Stage:	Main sequence	Red giant	Horizontal branch	Planetary nebula	White dwarf
Sun's age:	4.5 Ga (now)	12.2 Ga	12.3 Ga	12.3305 Ga	12.3306 Ga

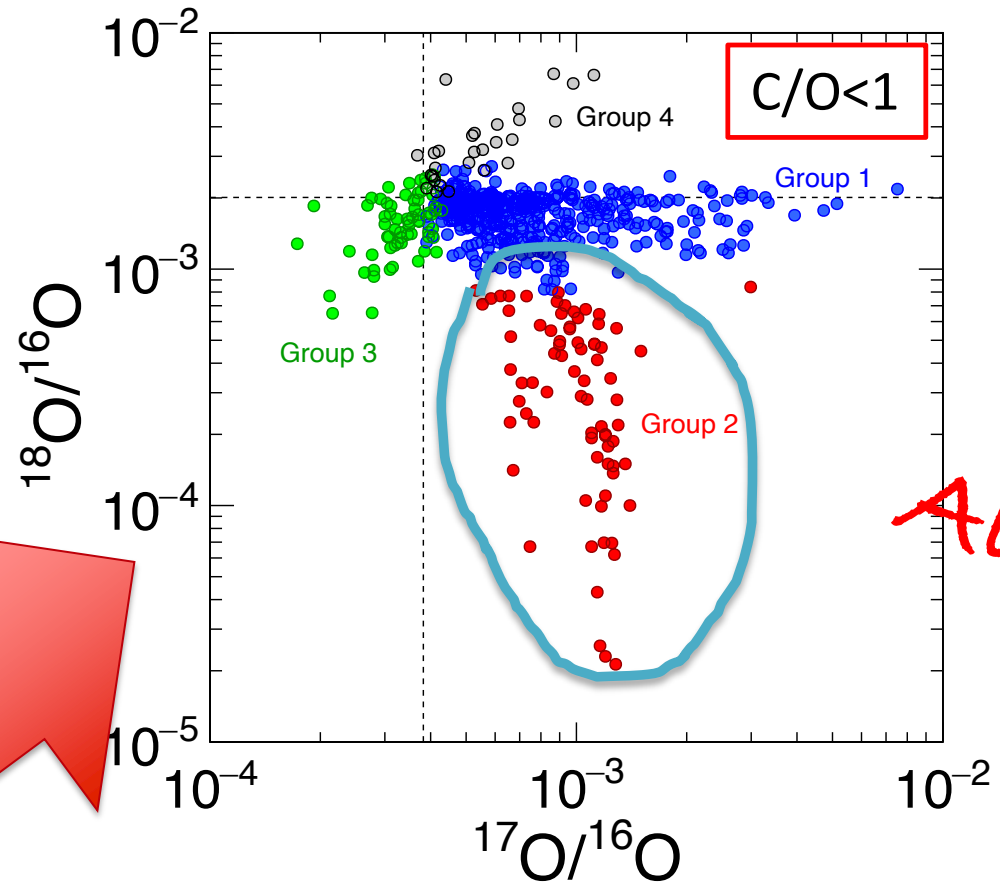
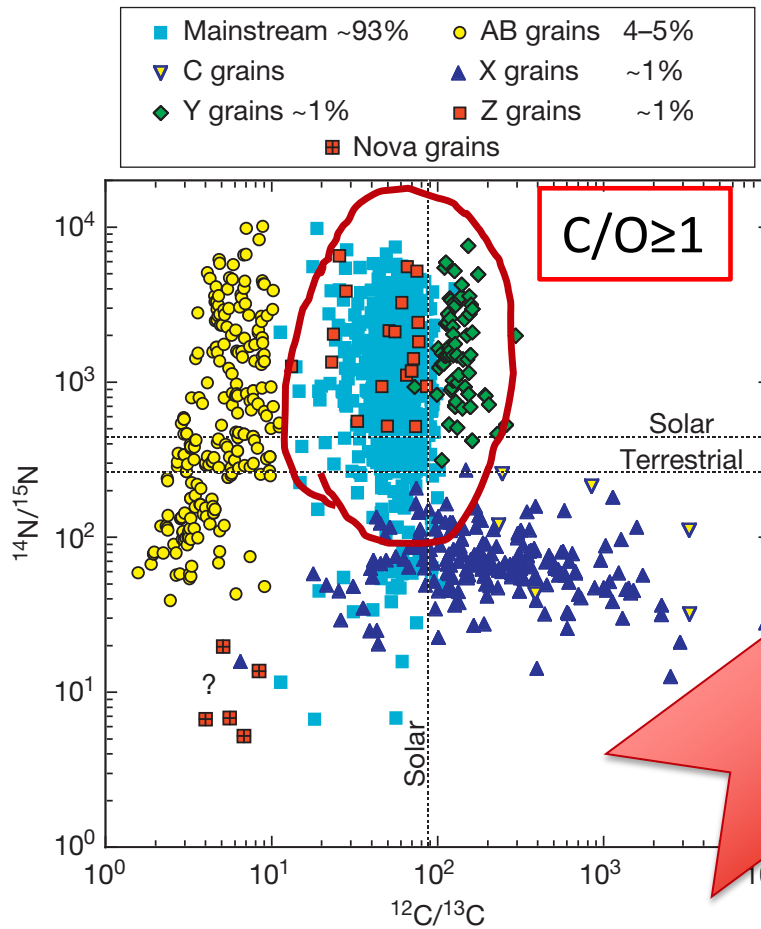


Despite their low masses LMS are so numerous to contribute for 75% to the total mass return from stars to the ISM (Sedlmayr 1994);





Presolar grains from AGB stars



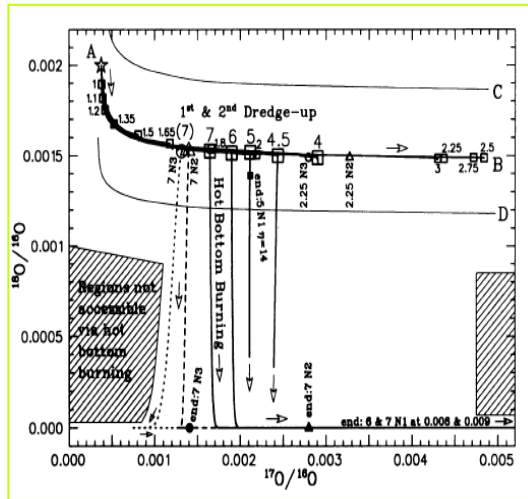
Al_2O_3

Presolar grains from AGB stars

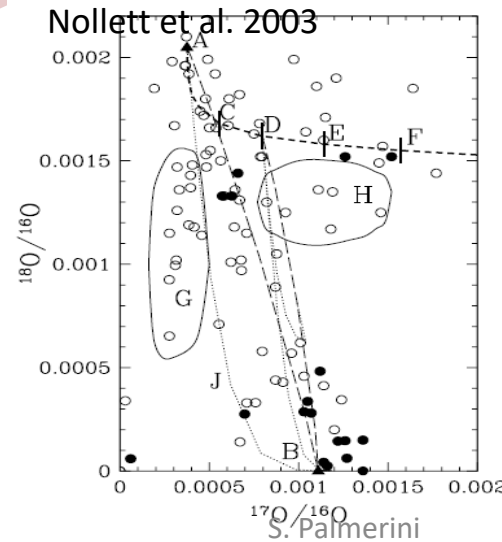
Oxide grains of AGB origin: HBB or CBP?

In conclusion, the measured $^{17}\text{O}/^{16}\text{O}$ ratio of grain OC2 ($= 1.25 \pm 0.07 \times 10^{-3}$) could be reproduced within the large error bars of the NACRE compilation ($2.44_{-1.78}^{+1.54} \times 10^{-3}$) in models of massive AGB stars; however, the much more precise $^{16}\text{O}(p,\gamma)^{17}\text{F}$ rate of the present work leads to $2.52_{-0.76}^{+0.88} \times 10^{-3}$ for the $^{17}\text{O}/^{16}\text{O}$ ratio and disagrees with the measured value. Consequently, there is not clear evidence to date for any stellar grain origin from massive AGB stars. Stellar model uncertain-

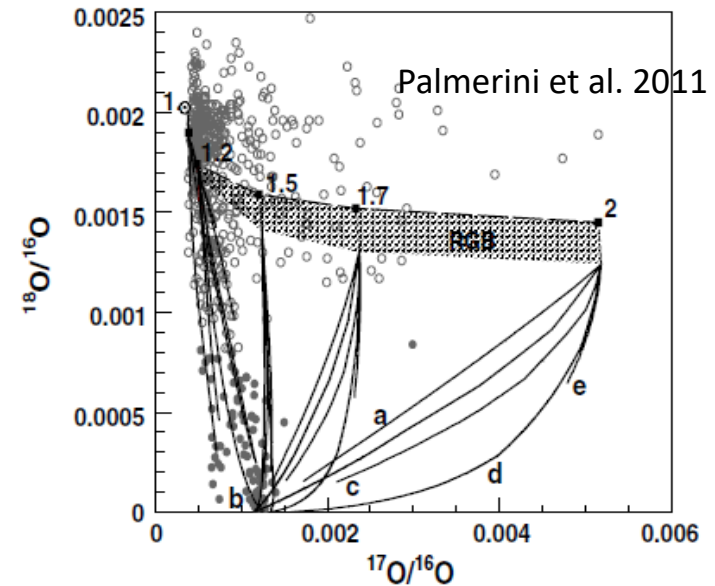
Iliadis et al 2008



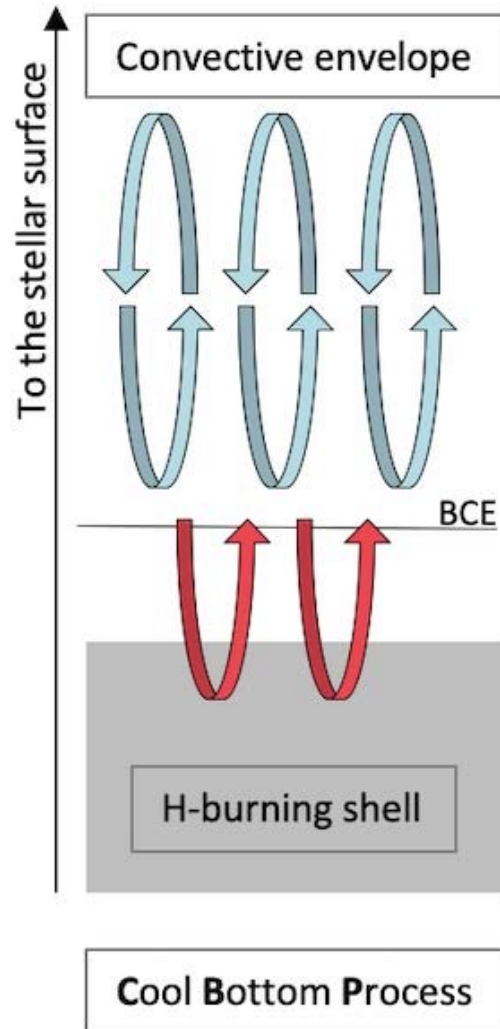
Boothroyd,
Sackmann &
Wasserburg 1995



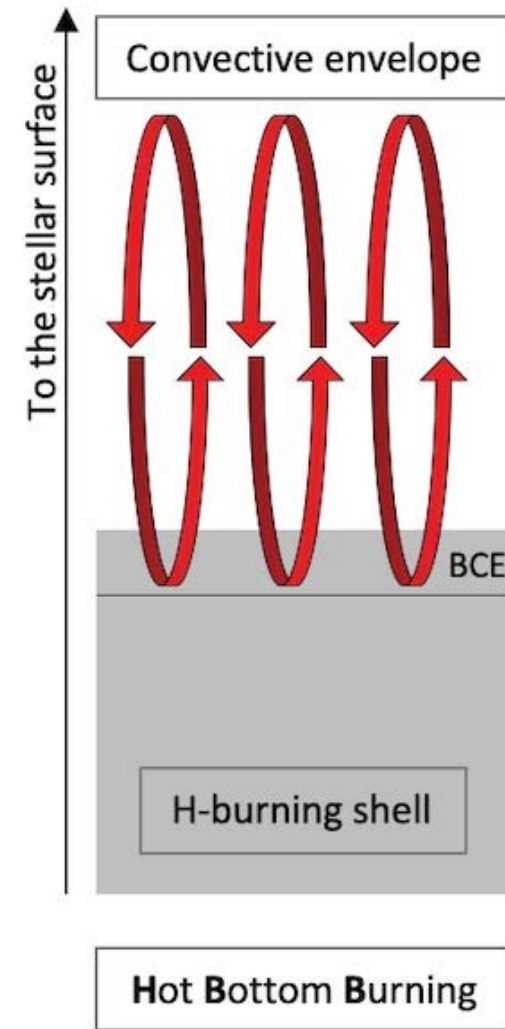
S. Palmerini



Cool Bottom Process ○ Hot Bottom Burning



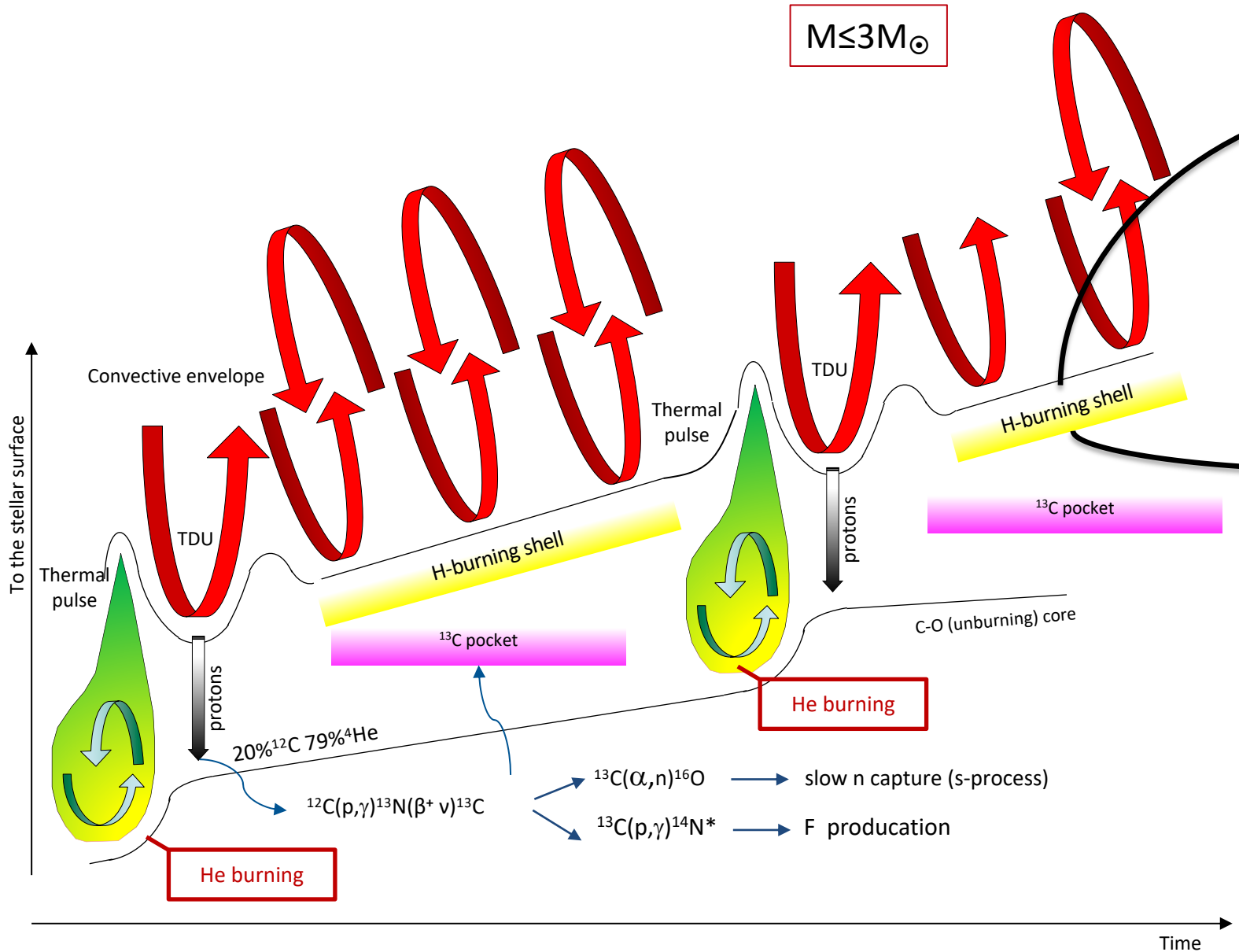
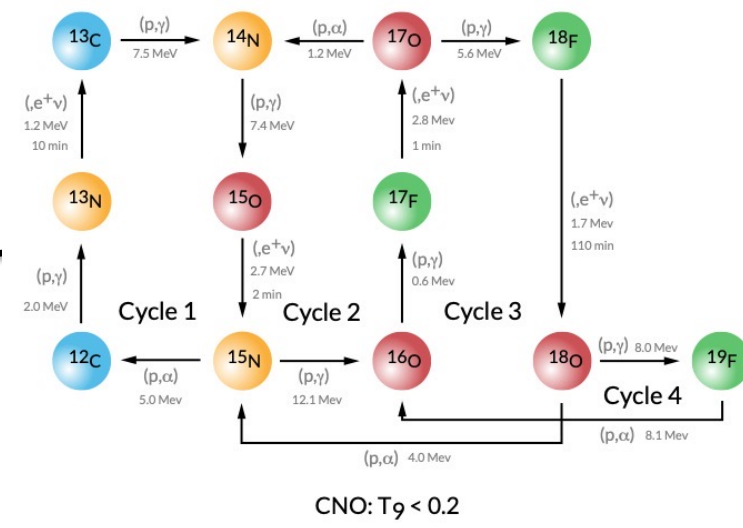
Low mass AGB stars



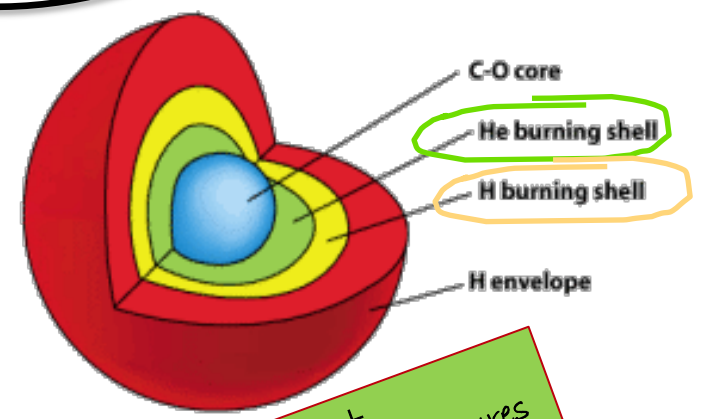
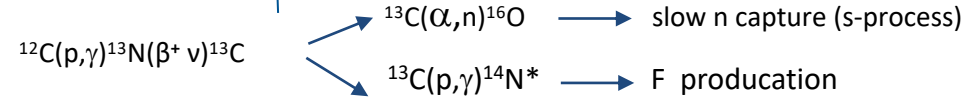
Intermediate mass AGB stars

HOW DOES AN AGB STAR WORK?

$M \leq 3M_{\odot}$



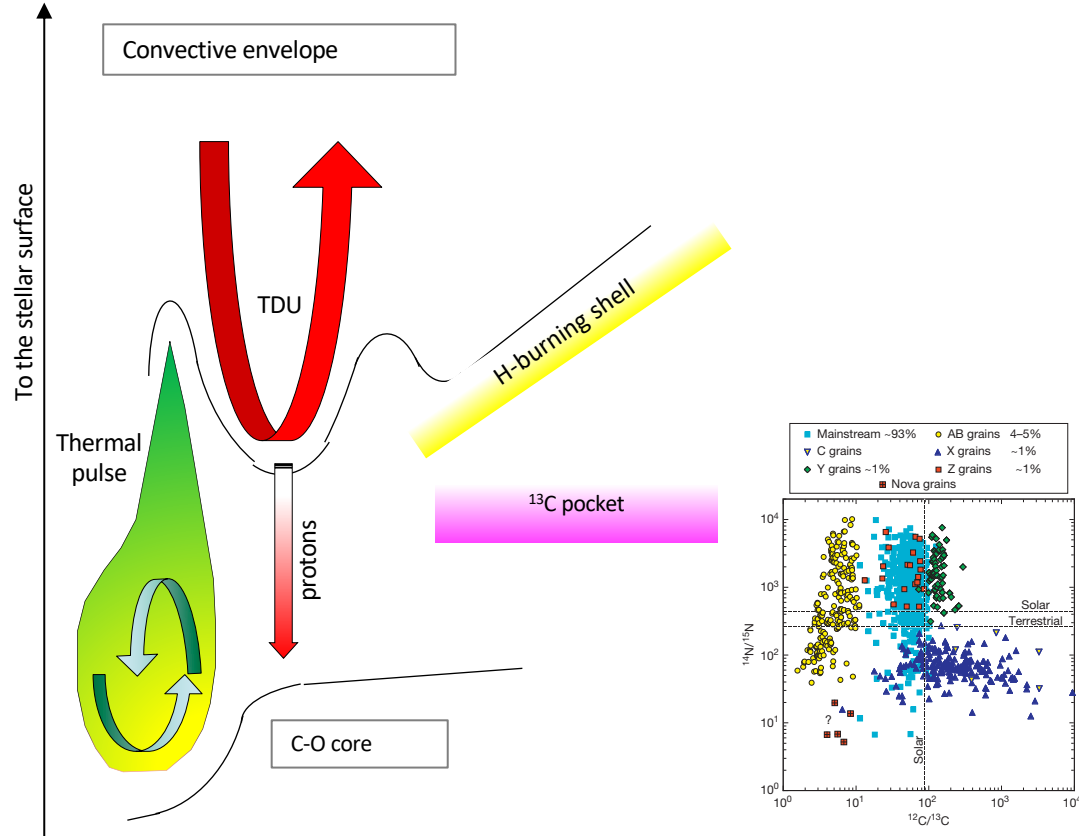
20% ^{12}C 79% ^4He



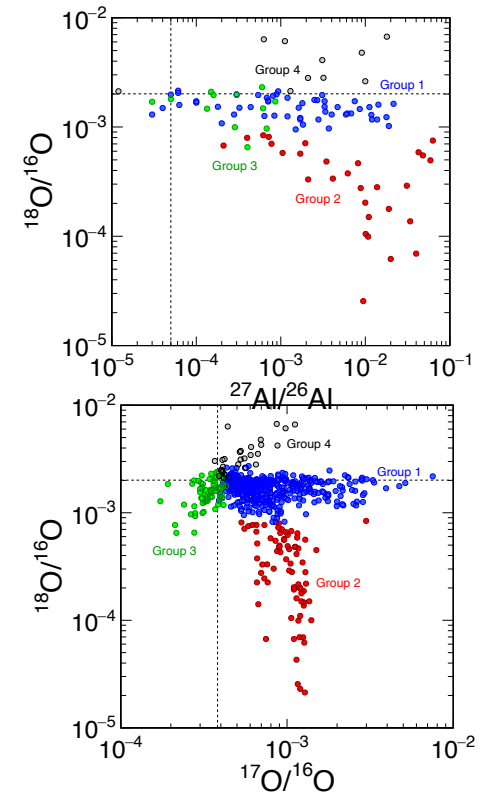
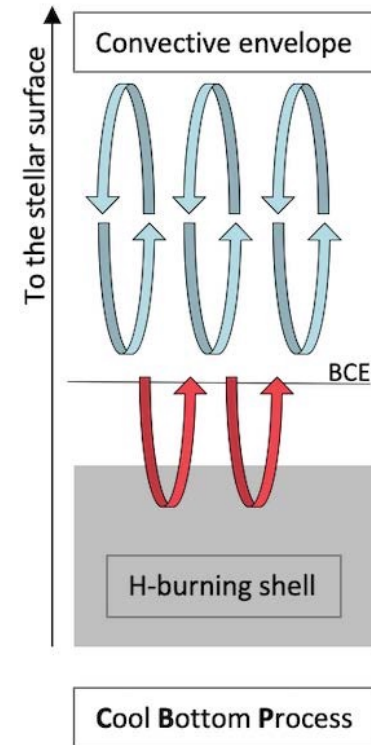
+ slow neutron captures s-process

THE MIXING MECHANISM WE ARE LOOKING HAS TO ACCOUNT FOR

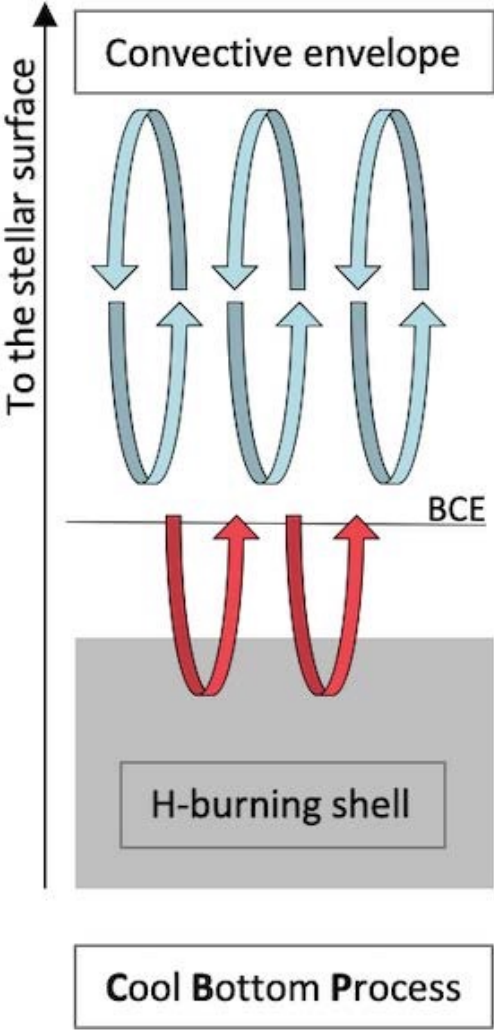
1. the formation of the ^{13}C pocket, whose resulting s-process nucleosynthesis reproduces the isotopic abundances in MS-SiC grains



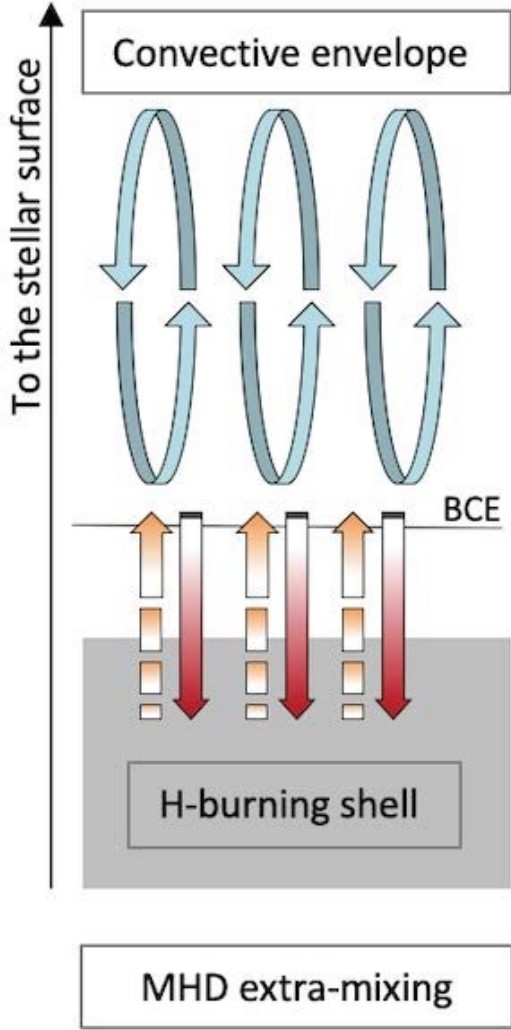
2. a deep (non convective) mixing accounting for the large ^{18}O depletion and ^{26}Al enrichment found in group 2 oxide grains



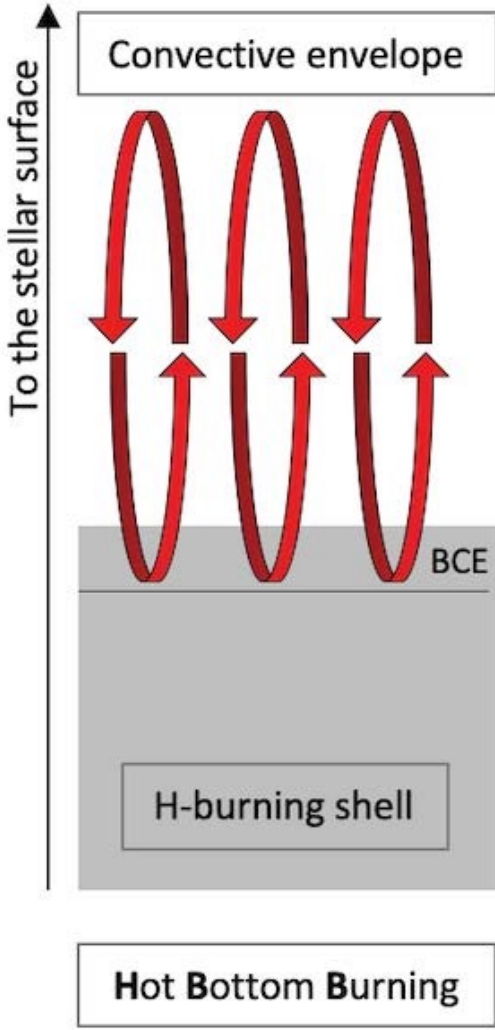
Cool Bottom Process, Bottom-up mixing or Hot Bottom Burning



Low mass AGB stars

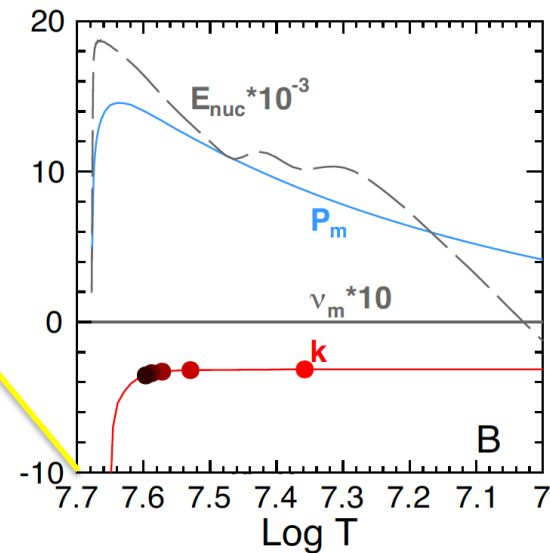
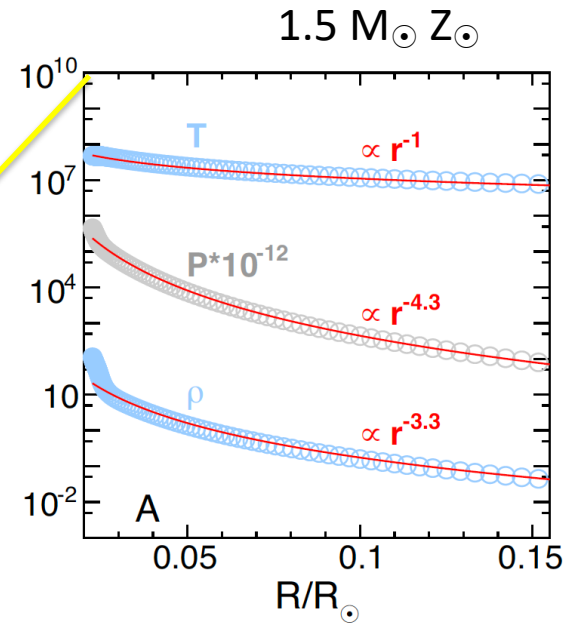
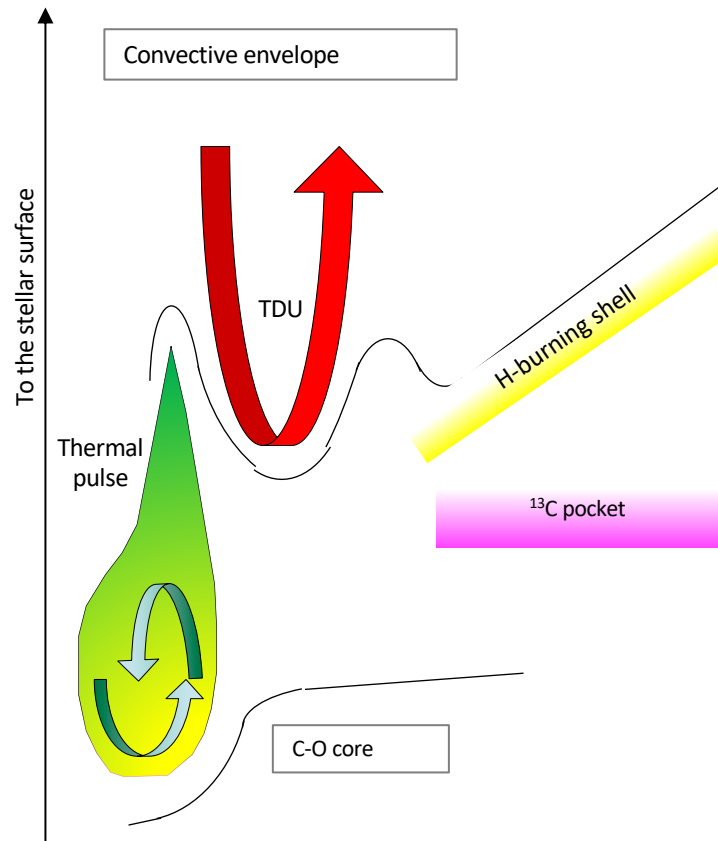


Low mass AGB stars



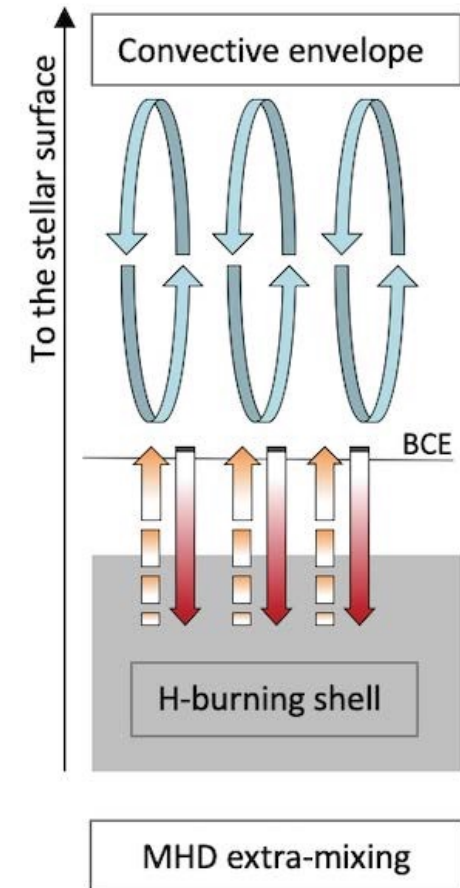
Intermediate mass AGB stars

IN THE RADIATIVE LAYERS BETWEEN THE BCE AND THE H-BURNING SHELL

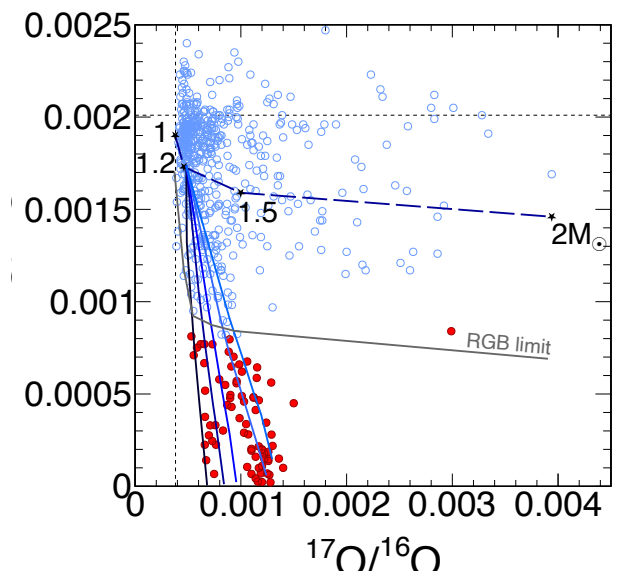
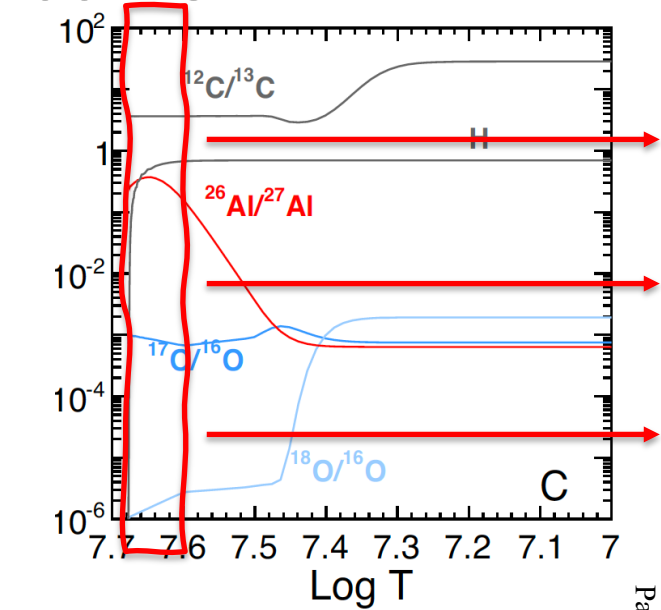
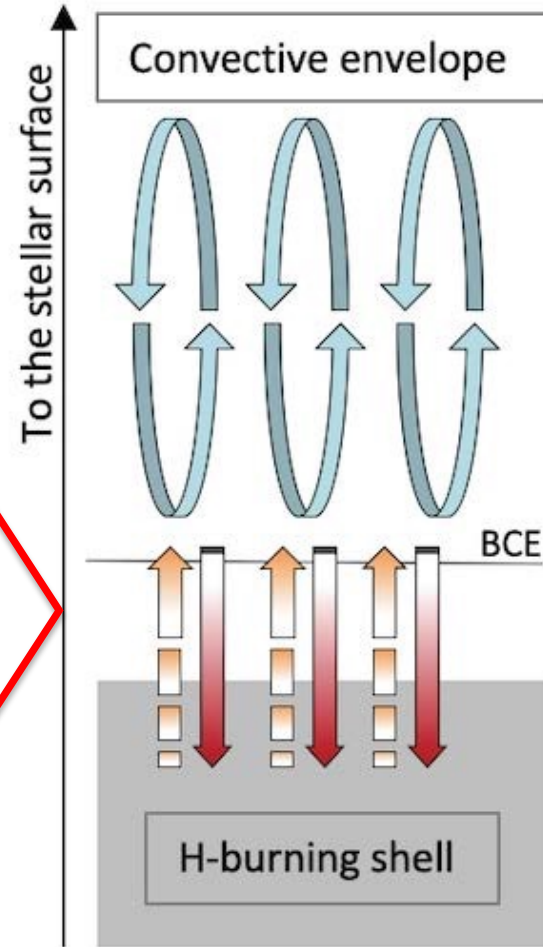
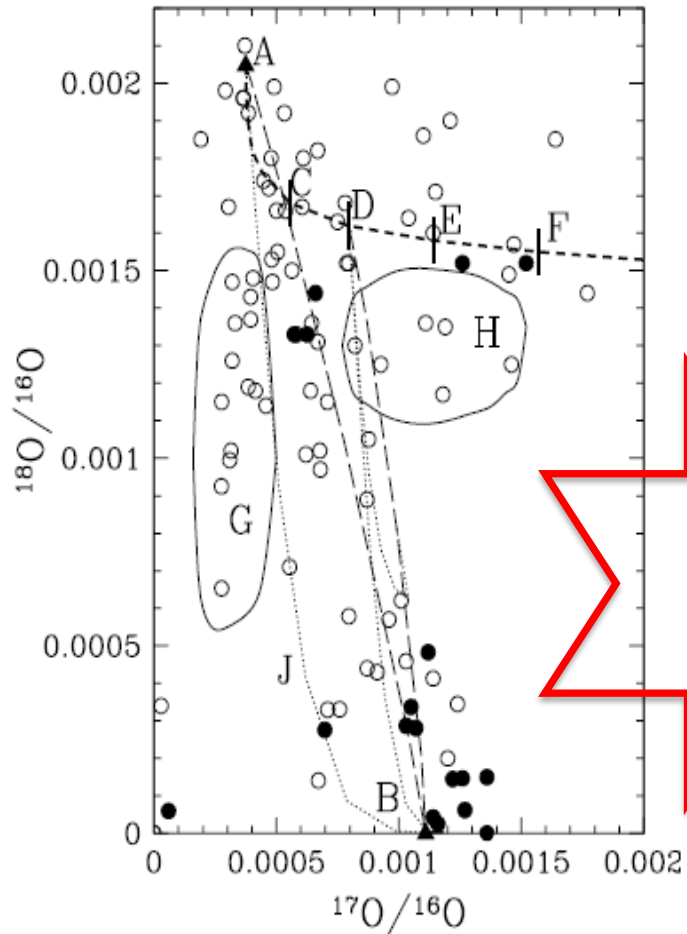
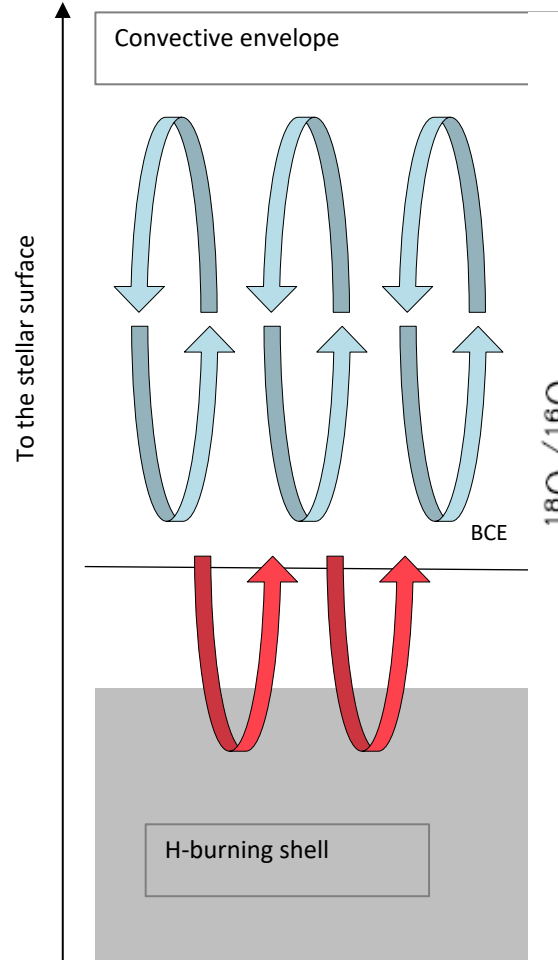


FROM THE MHD MODEL
BY NUCCI & BUSSO 2014
(*ApJ*, 787, 141 2014)

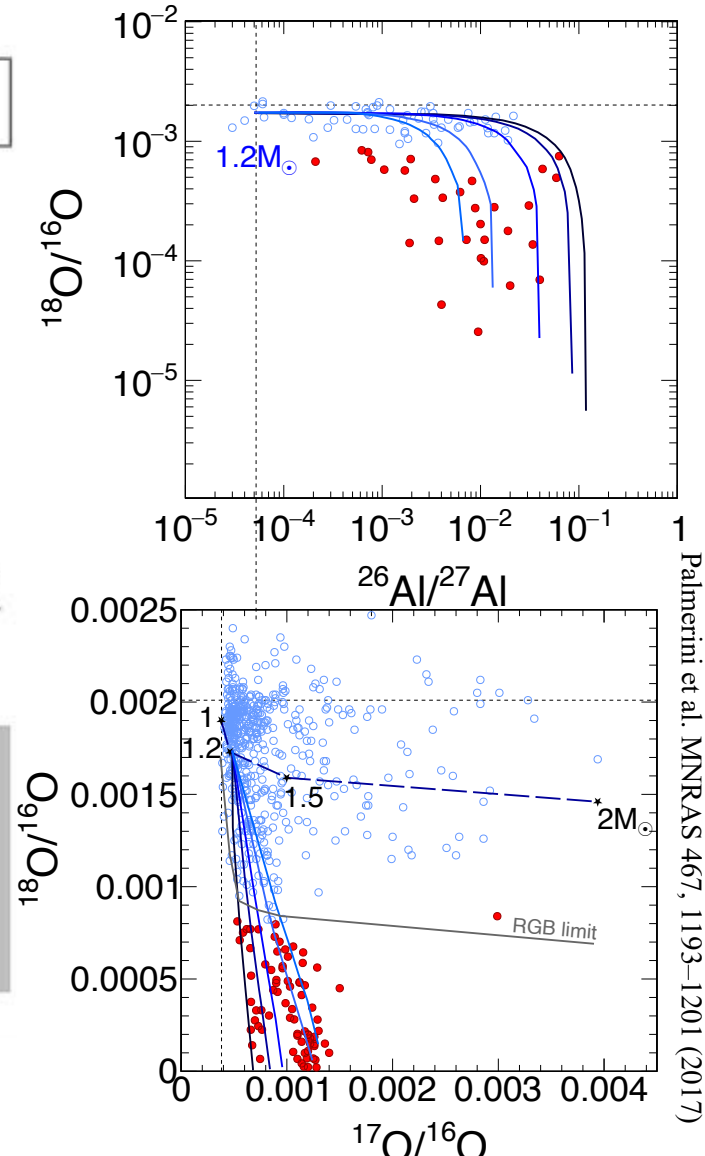
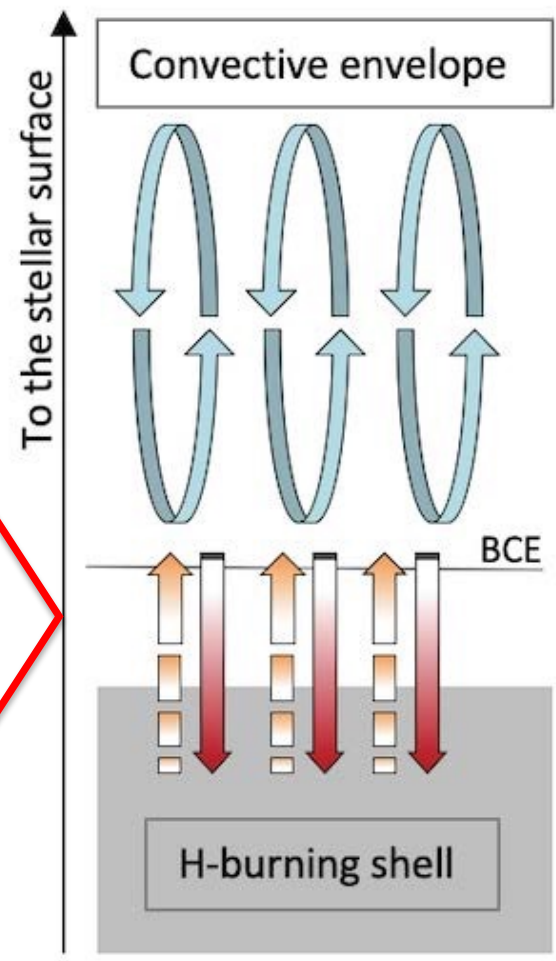
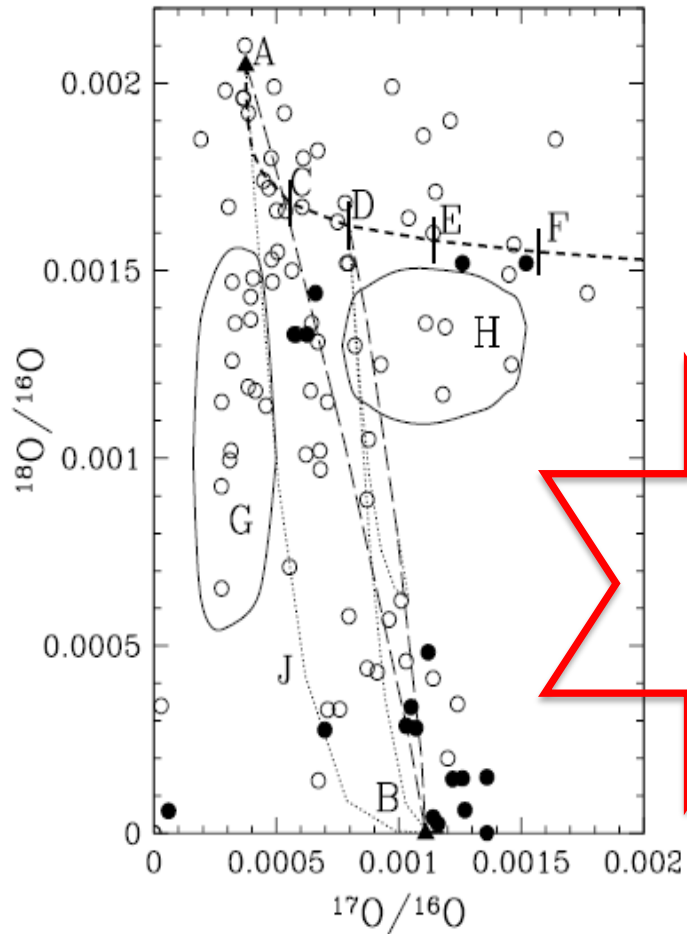
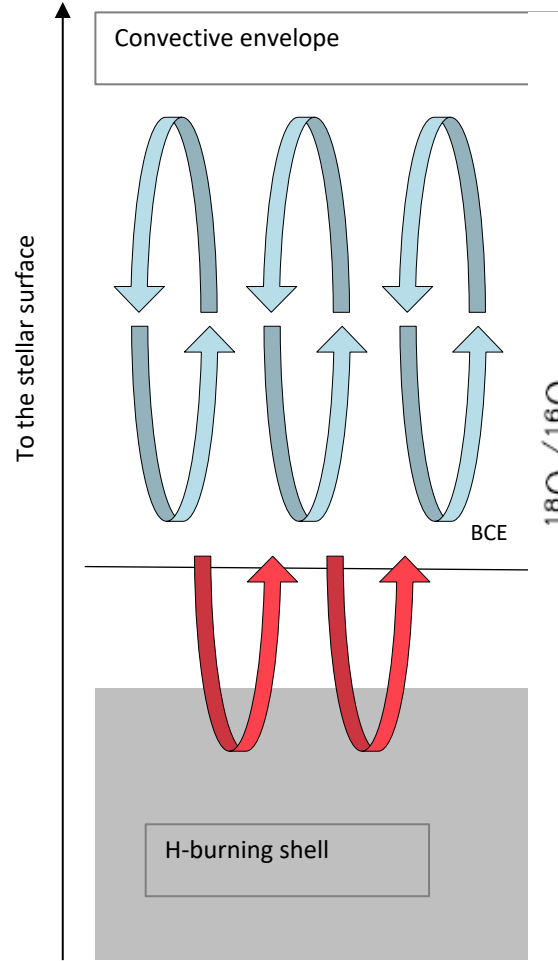
$$v_r = v_P \left(\frac{r_P}{r} \right)^{-(k+1)}$$



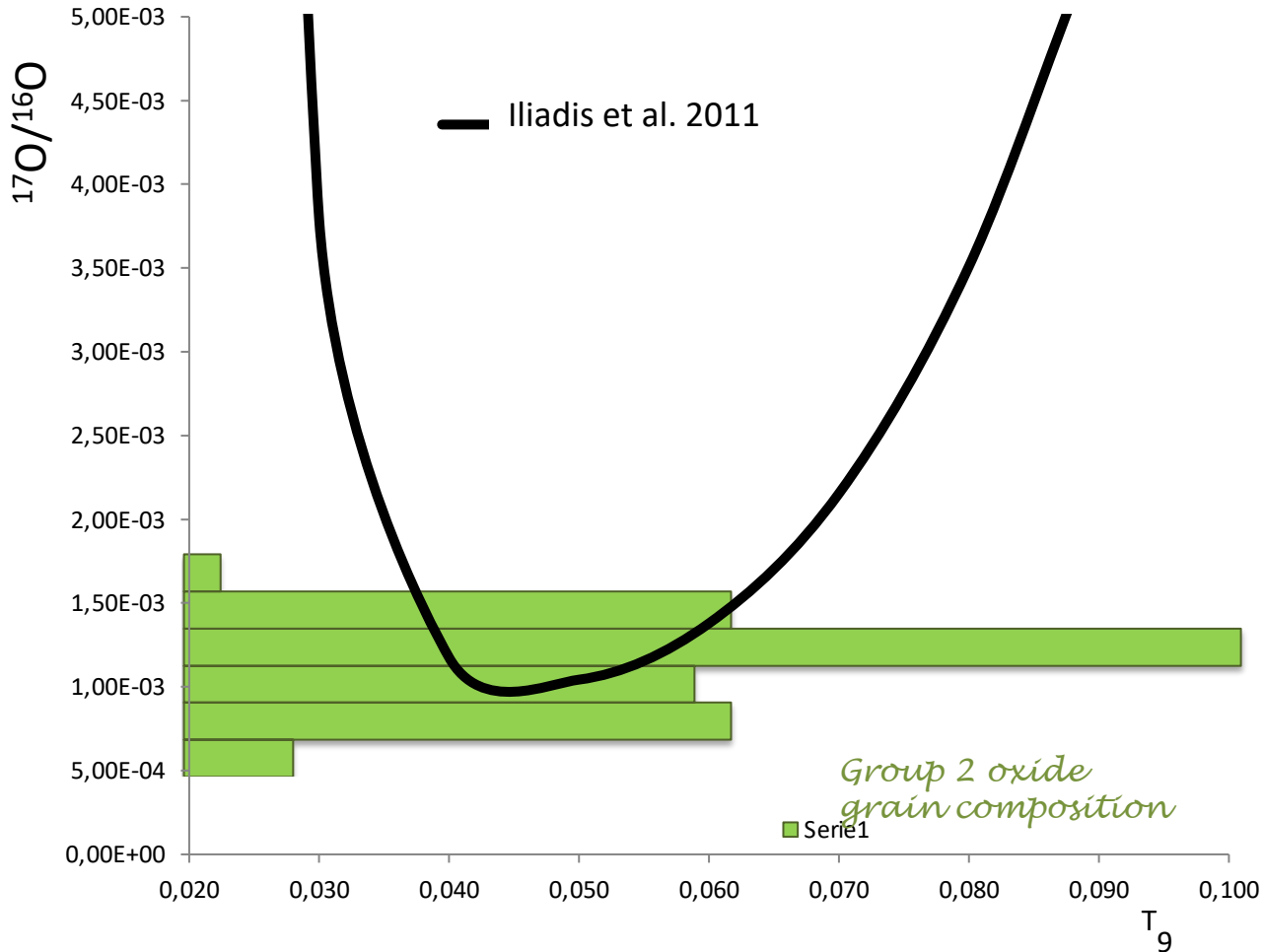
From CBP to a Bottom-up mixing (MHD and advective) in low mass stars



From CBP to a Bottom-up mixing (MHD and advective) in low mass stars



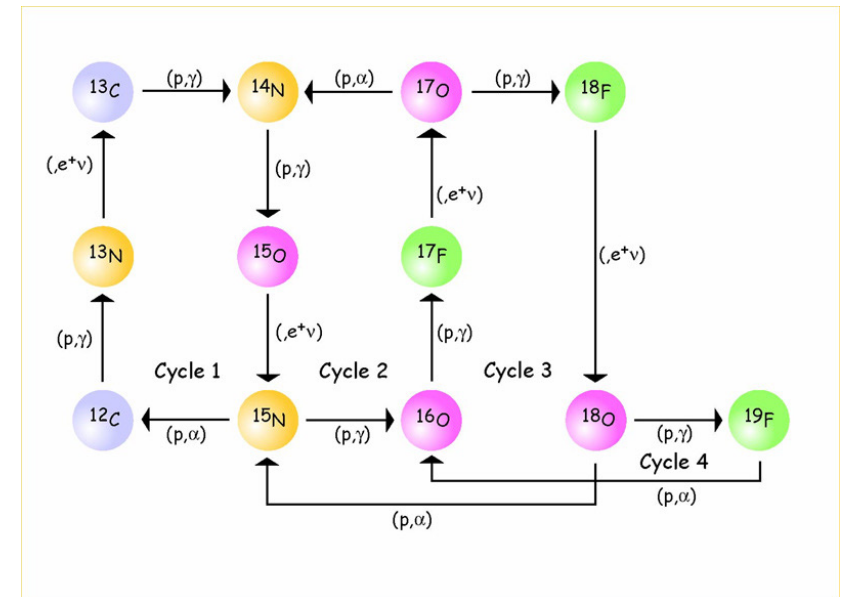
$^{17}\text{O}(p,\alpha)^{14}\text{N}$ rate and the $^{17}\text{O}/^{16}\text{O}$ equilibrium values



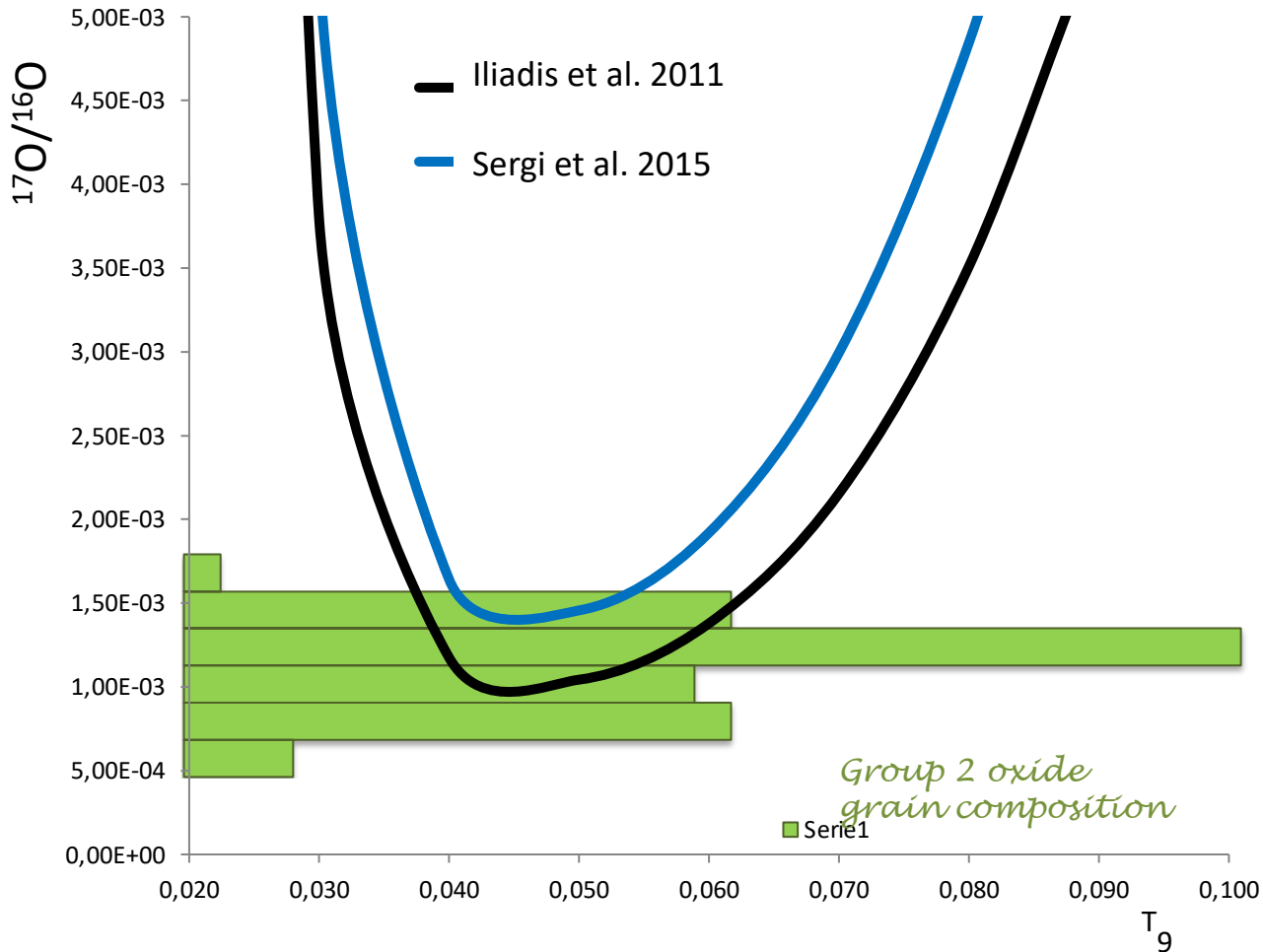
$$\frac{dY_{^{17}\text{O}}}{dt} = Y_{^{16}\text{O}} Y_H N_A \langle \sigma v \rangle_{^{16}\text{O}(p,\gamma)^{17}\text{F}} \rho - Y_{^{17}\text{O}} Y_H N_A \left(\langle \sigma v \rangle_{^{16}\text{O}(p,\gamma)^{17}\text{F}} + \langle \sigma v \rangle_{^{16}\text{O}(p,\alpha)^{14}\text{N}} \right)$$

$$\frac{Y_{^{16}\text{O}}}{Y_{^{17}\text{O}}} = \frac{N_A \langle \sigma v \rangle_{^{17}\text{O}(p,\gamma)^{18}\text{F}} + N_A \langle \sigma v \rangle_{^{17}\text{O}(p,\alpha)^{14}\text{N}}}{N_A \langle \sigma v \rangle_{^{16}\text{O}(p,\gamma)^{17}\text{F}}}$$

Equilibrium conditions



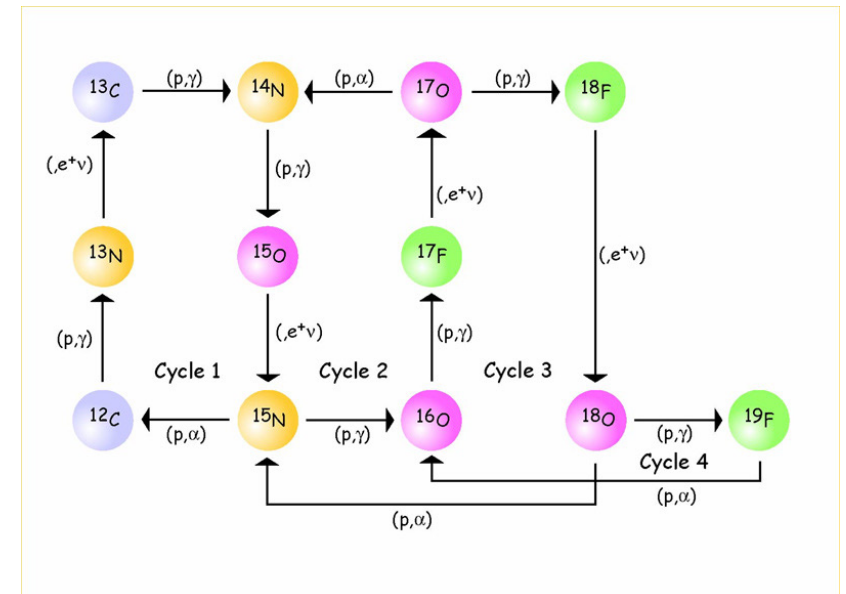
$^{17}\text{O}(p,\alpha)^{14}\text{N}$ rate and the $^{17}\text{O}/^{16}\text{O}$ equilibrium values



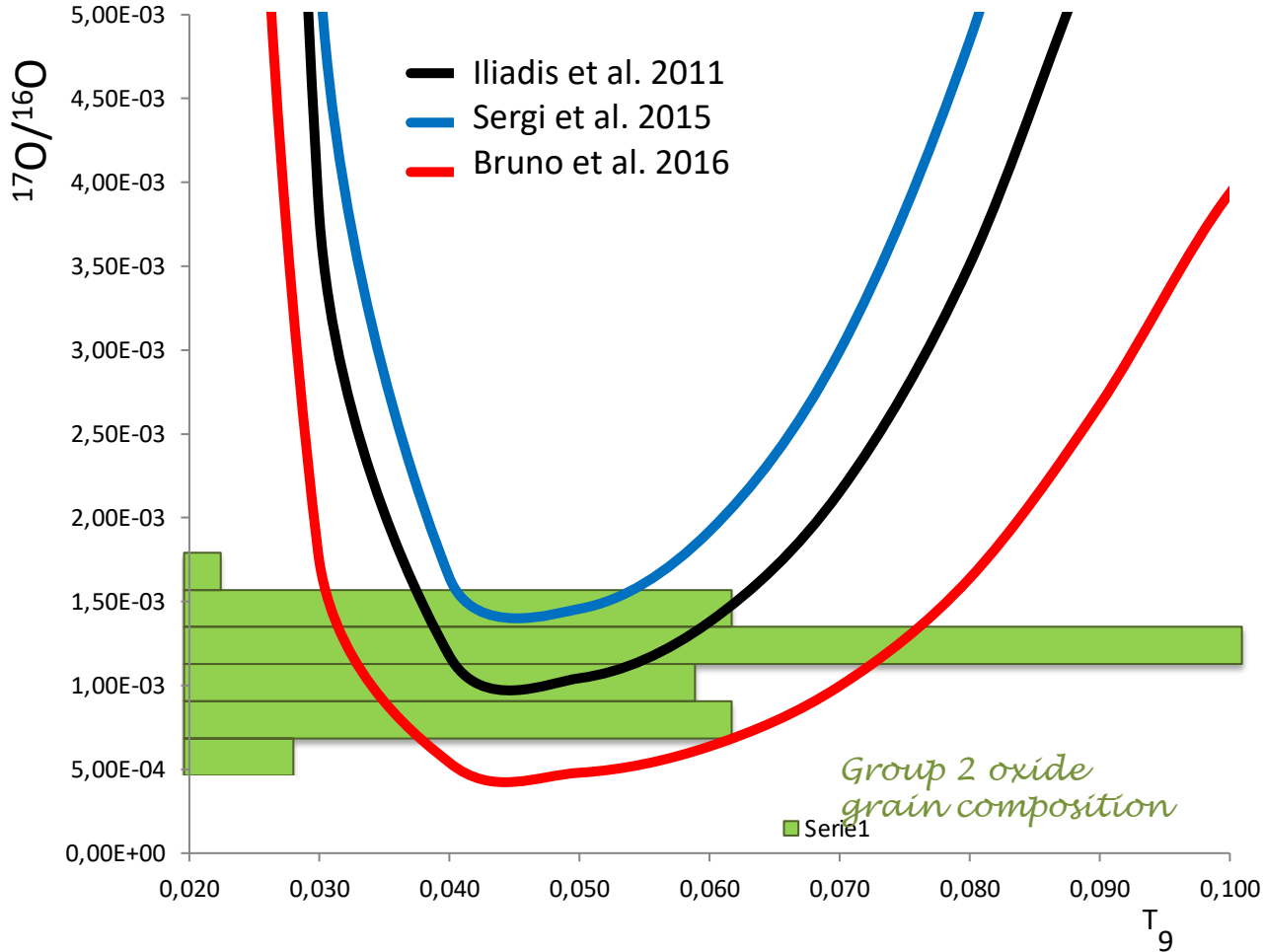
$$\frac{dY_{^{17}\text{O}}}{dt} = Y_{^{16}\text{O}} Y_H N_A \langle \sigma v \rangle_{^{16}\text{O}(p,\gamma)^{17}\text{F}} \rho - Y_{^{17}\text{O}} Y_H N_A \left(\langle \sigma v \rangle_{^{16}\text{O}(p,\gamma)^{17}\text{F}} + \langle \sigma v \rangle_{^{16}\text{O}(p,\alpha)^{14}\text{N}} \right)$$

$$Y_{^{16}\text{O}} = \frac{N_A \langle \sigma v \rangle_{^{17}\text{O}(p,\gamma)^{18}\text{F}} + N_A \langle \sigma v \rangle_{^{17}\text{O}(p,\alpha)^{14}\text{N}}}{N_A \langle \sigma v \rangle_{^{16}\text{O}(p,\gamma)^{17}\text{F}}}$$

Equilibrium conditions



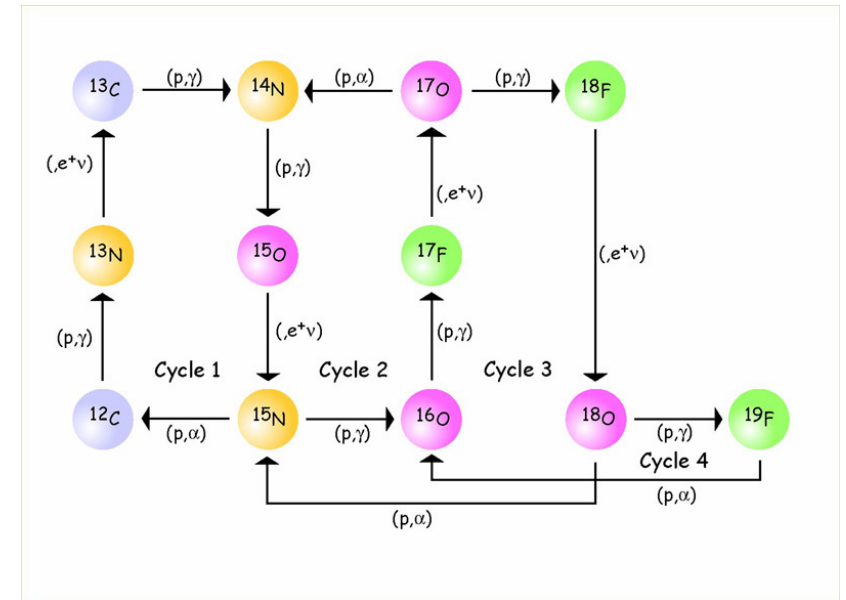
$^{17}\text{O}(p,\alpha)^{14}\text{N}$ rate and the $^{17}\text{O}/^{16}\text{O}$ equilibrium values



$$\frac{dY_{^{17}\text{O}}}{dt} = Y_{^{16}\text{O}} Y_H N_A \langle \sigma v \rangle_{^{16}\text{O}(p,\gamma)^{17}\text{F}} \rho - Y_{^{17}\text{O}} Y_H N_A \left(\langle \sigma v \rangle_{^{16}\text{O}(p,\gamma)^{17}\text{F}} + \langle \sigma v \rangle_{^{16}\text{O}(p,\alpha)^{14}\text{N}} \right)$$

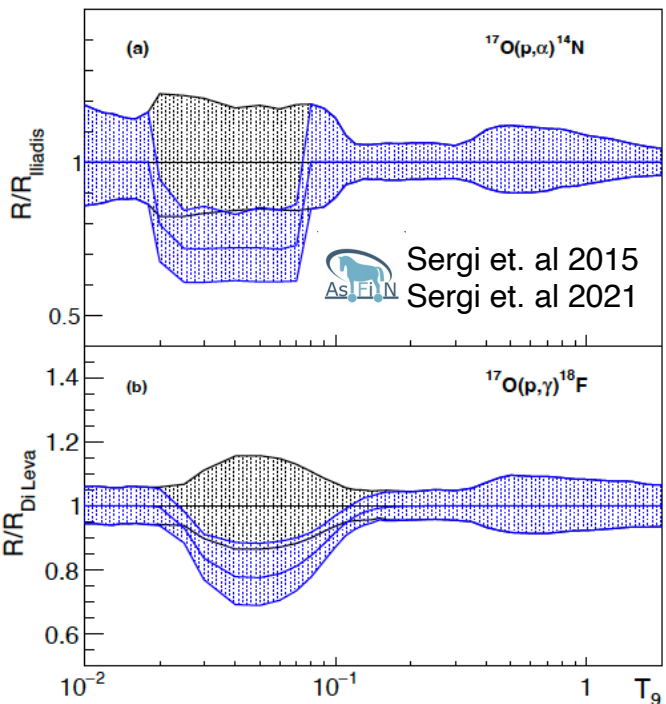
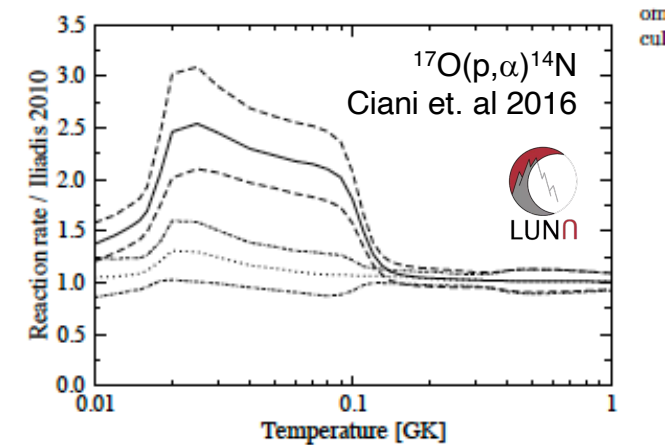
$$Y_{^{16}\text{O}} = \frac{N_A \langle \sigma v \rangle_{^{17}\text{O}(p,\gamma)^{18}\text{F}} + N_A \langle \sigma v \rangle_{^{17}\text{O}(p,\alpha)^{14}\text{N}}}{N_A \langle \sigma v \rangle_{^{16}\text{O}(p,\gamma)^{17}\text{F}}}$$

Equilibrium conditions



$^{17}\text{O}(p,\alpha)^{14}\text{N}$ resonances relevant for Astrophysics

$\omega\gamma$ (eV)	Bruno et al. 2016	Sergi et al. 2015 THM	Iliadis et al. 2010	NACRE
65 keV	$10.0 \pm 1.1 \cdot 10^{-9}$	$3.4 \pm 0.6 \cdot 10^{-9}$	$4.7 \pm 0.8 \cdot 10^{-9}$	$5.5^{+1.8}_{-1.0} \cdot 10^{-9}$
183 keV	$1.66 \pm 0.1 \cdot 10^{-3}$	$1.16 \pm 0.1 \cdot 10^{-3}$	$1.66 \pm 0.1 \cdot 10^{-3}$	$5.8^{+5.2}_{-5.8} \cdot 10^{-5}$



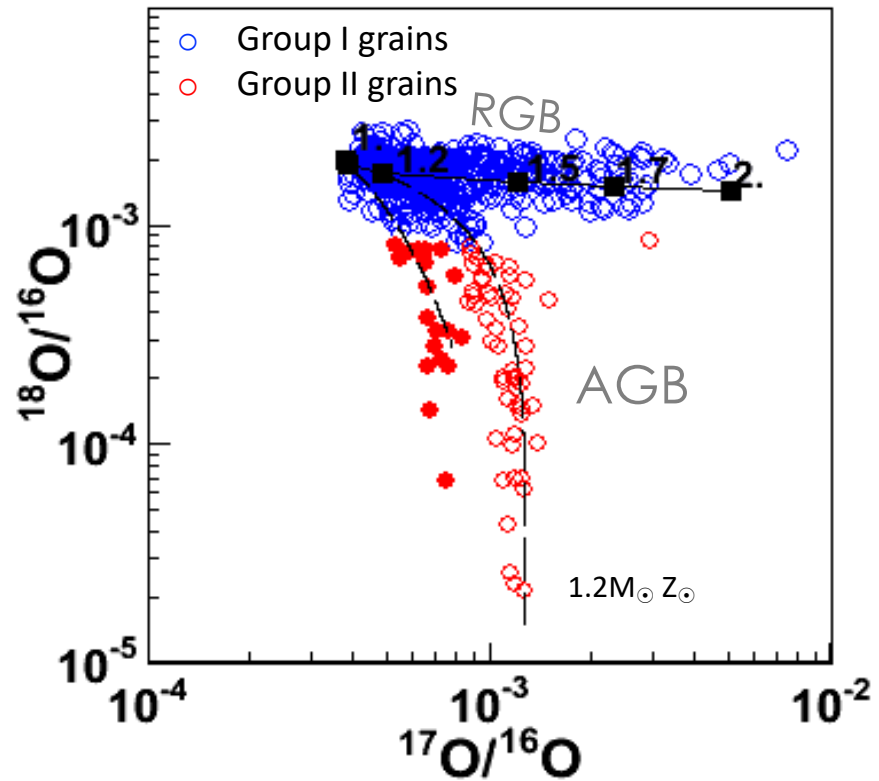
At H-burning temperatures the (p, α) channel dominates, being its rate up to 2 order of magnitude larger than the (p, γ) one

$^{17}\text{O}(p,\gamma)^{18}\text{F}$ resonances relevant for Astrophysics

$\omega\gamma$ (eV)	Piatti NPAX Ciani NICXVI	Buckner et al 2015	Sergi et al. 2015 *scaled	Iliadis et al. 2010
65 keV	$7.8 \pm 0.8 \cdot 10^{-11}$	$1.6 \pm 0.3 \cdot 10^{-11}$ eV	$1.18 \pm 0.22 \cdot 10^{-11}$	$1.64 \pm 0.28 \cdot 10^{-11}$

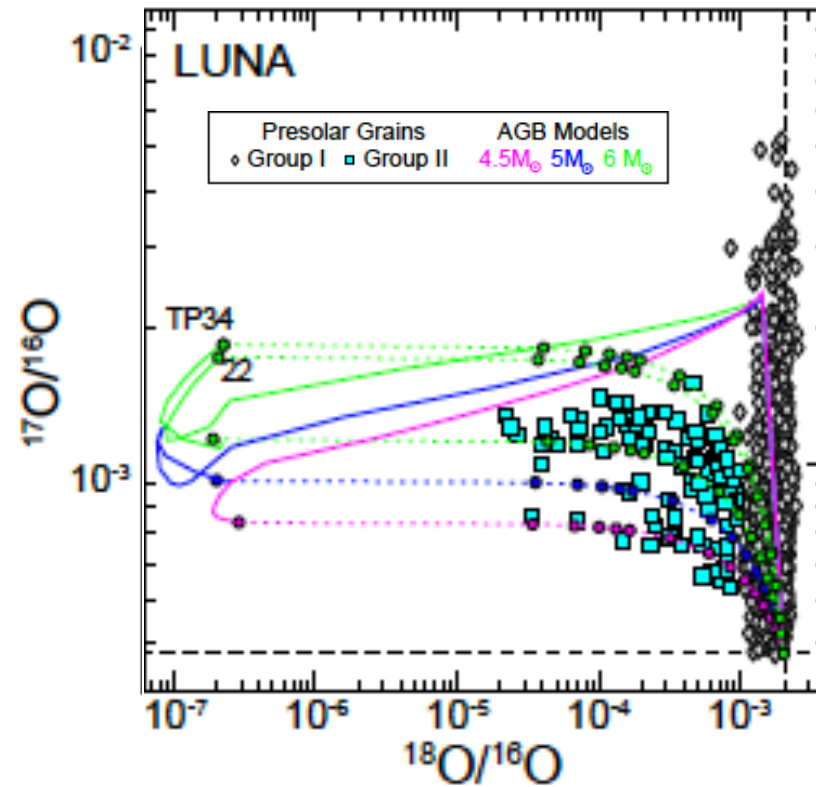
Grains vs B-UP and Grains vs HBB

...of low mass with BUP mixing and $^{17}\text{O}(p,\alpha)^{14}\text{N}$ rate by Sergi et al 2015



Palmerini et al. 2014

...of intermediate mass with HBB and $^{17}\text{O}(p,\alpha)^{14}\text{N}$ rate by Bruno et al 2016



Lugaro et al. 2017

Grains vs B-UP and Grains vs HBB

...of low mass with BUP mixing and $^{17}\text{O}(p,\alpha)^{14}\text{N}$ rate by Sergi et al 2015

...of intermediate mass with HBB and $^{17}\text{O}(p,\alpha)^{14}\text{N}$ rate by Bruno et al 2016

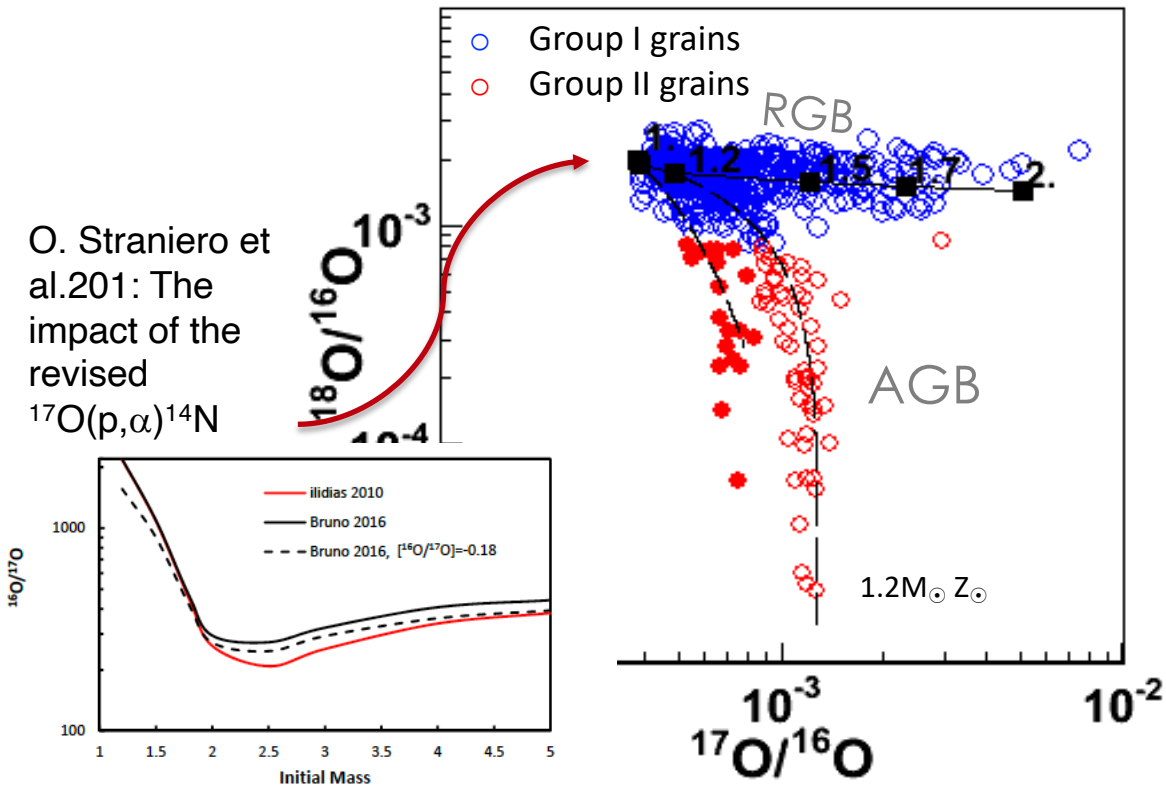
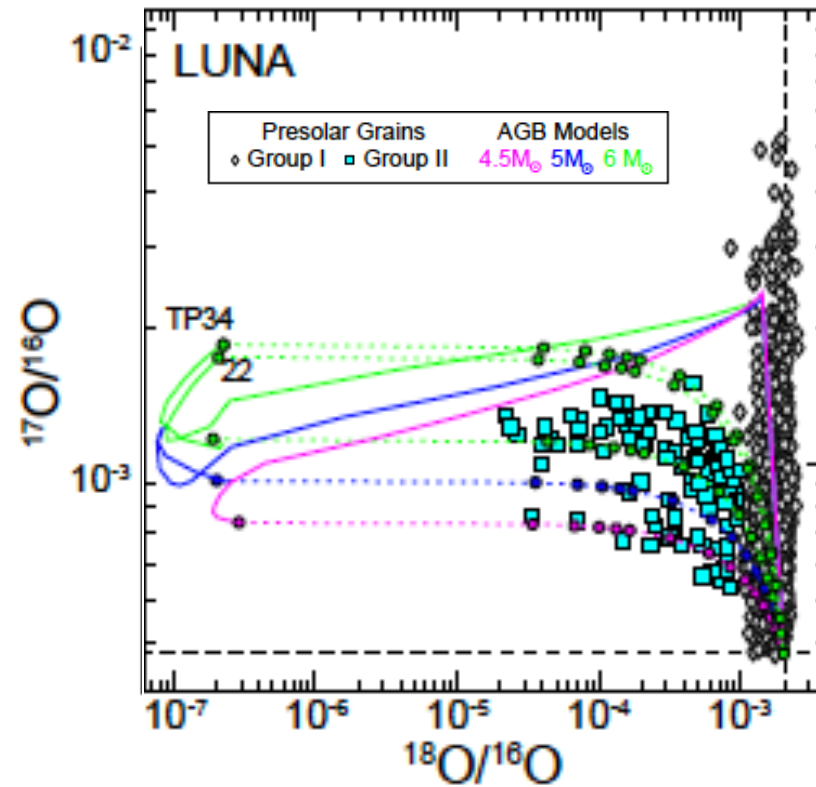


Fig. 3. Post-FDU $^{16}\text{O}/^{17}\text{O}$ at the surface of models with different initial mass and different rates and/or initial composition (see the legend).

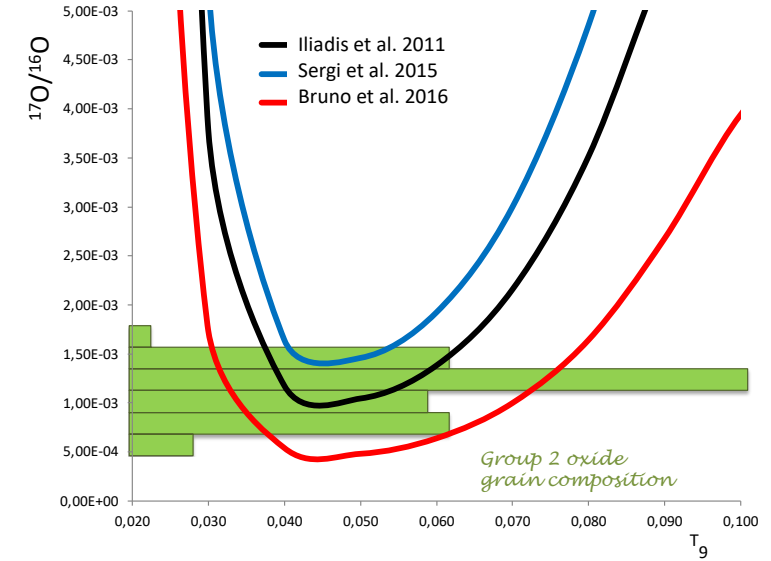
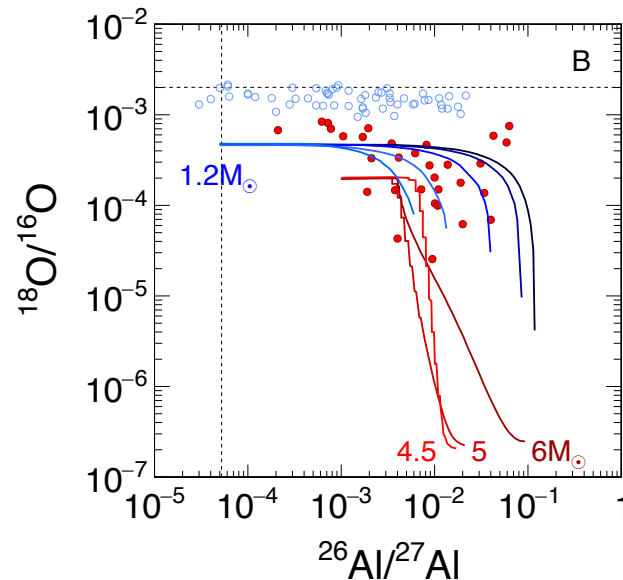
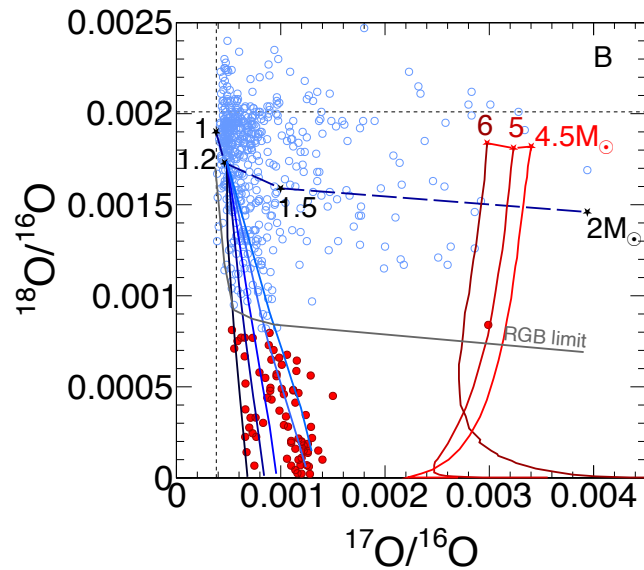
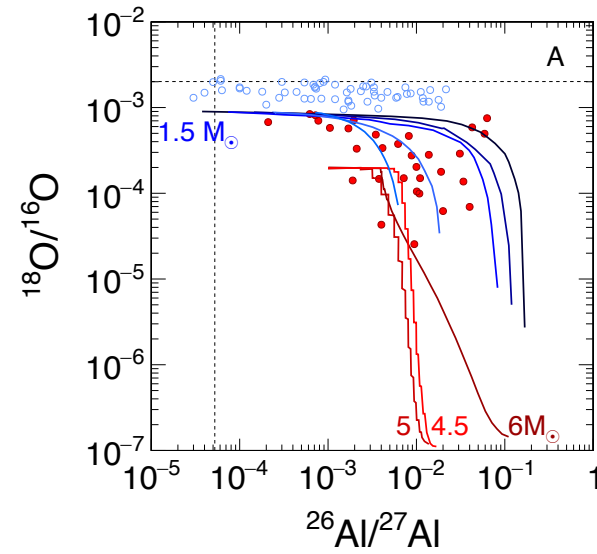
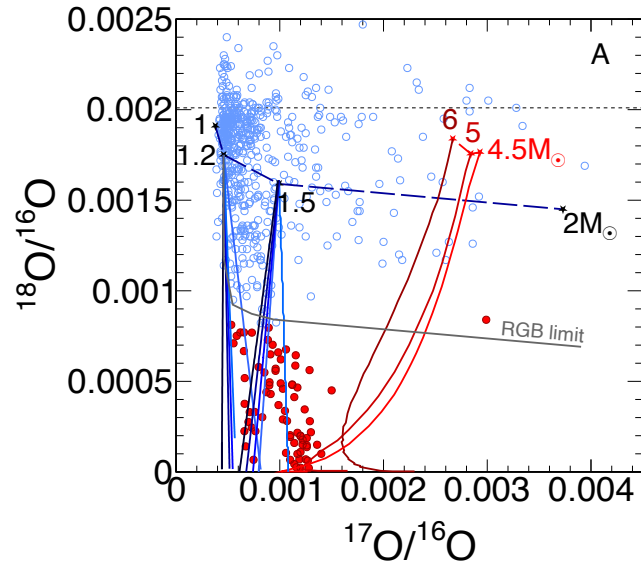
et al. 2014



Lugaro et al. 2017

MIX OR HBB? IS THIS A 'NUCLEAR' QUESTION?

Reaction	Set A	Set B
$^{18}\text{O}(p,\gamma)^{17}\text{F}$	Iliadis et al. (2010)	Iliadis et al. (2010)
$^{17}\text{O}(p,\alpha)^{14}\text{N}$	Bruno et al. (2016)	Sergi et al. (2015)
$^{17}\text{O}(p,\gamma)^{18}\text{F}$	Di Leva et al. (2014)	Sergi et al. (2015)
$^{18}\text{O}(p,\alpha)^{15}\text{N}$	Bruno et al. (2019)	La Cognata et al. (2010)
$^{18}\text{O}(p,\gamma)^{19}\text{F}$	Best et al. (2019)	Iliadis et al. (2010)
$^{25}\text{Mg}(p,\gamma)^{26}\text{Al}$	Straniero et al. (2013)	Straniero et al. (2013)
$^{26}\text{Al}(p,\gamma)^{27}\text{Si}$	Iliadis et al. (2010)	Iliadis et al. (2010)

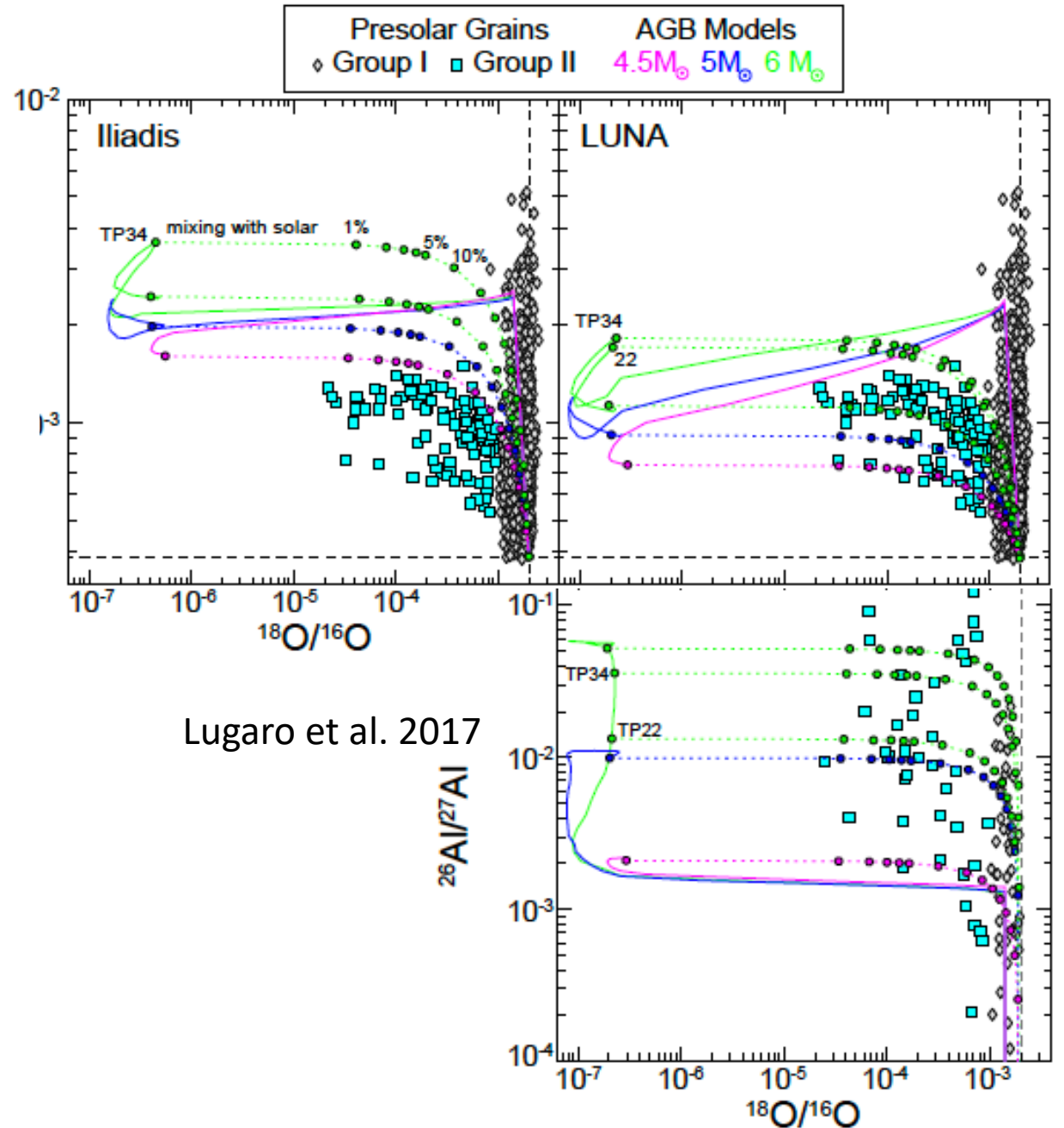
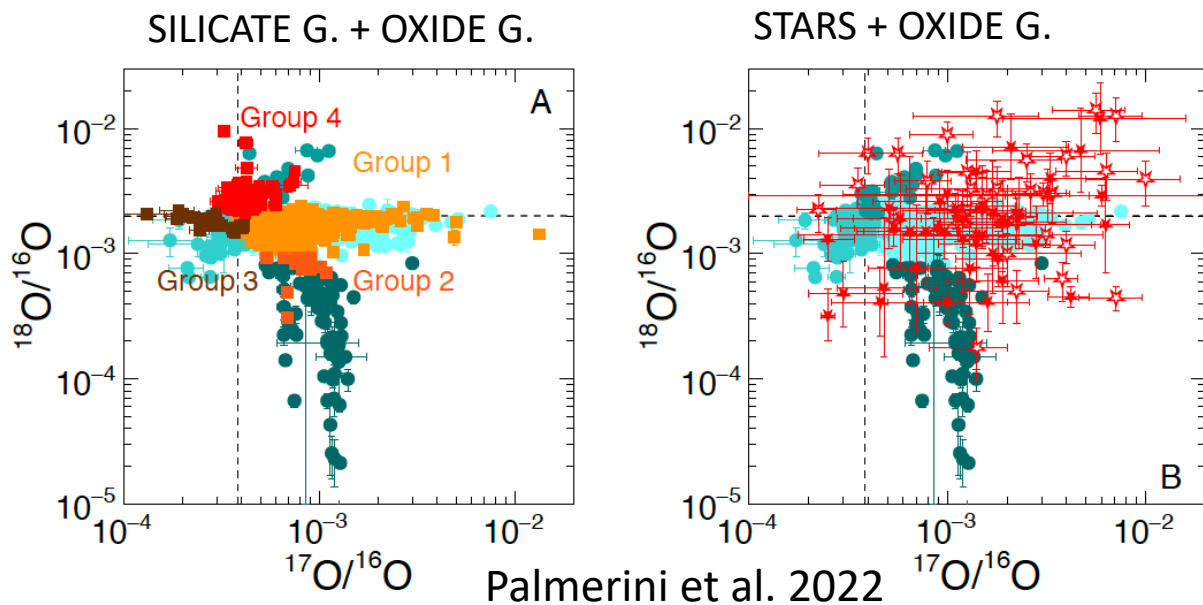


Magnetic mixing at play in low mass AGBs (1.2-1.5 M_{\odot}) provides in any case a match to group 2 oxide grains.

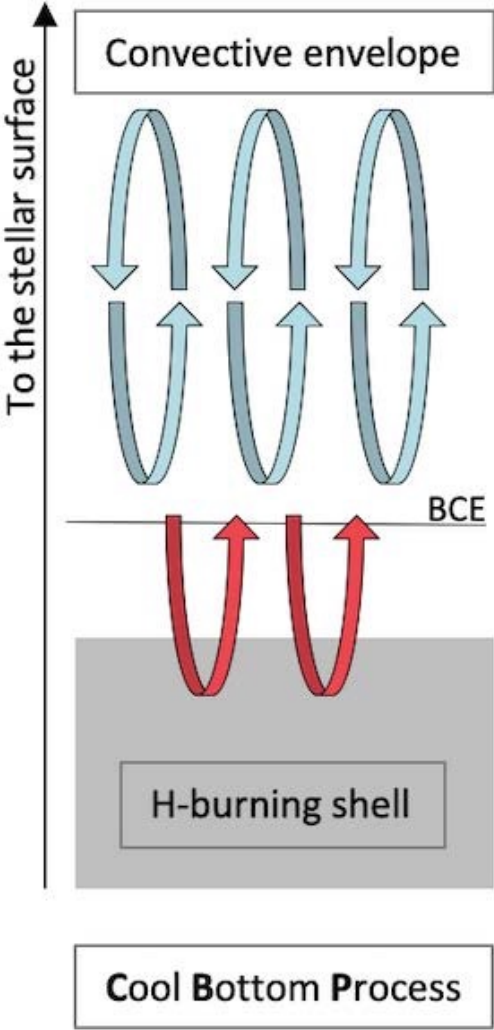
HBB in intermediate mass AGB models, reproduce a fraction of the grain sample only for one of the two nuclear data sets.

Hot Bottom Burning

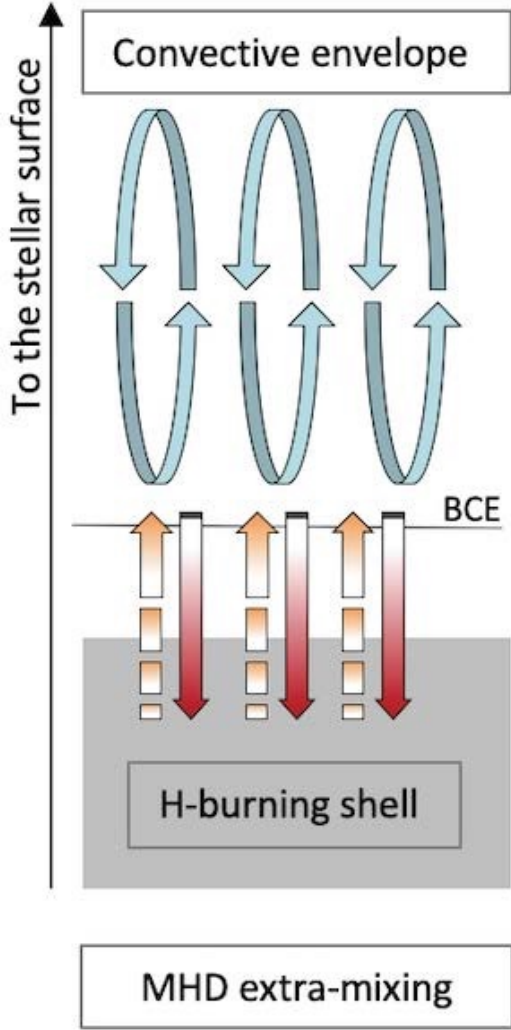
In case of AGB stars affected by HHB, the fit to grain abundances can be improved by using nuclear data by LUNA, but some dilution effects have to be added to have a full overlap between models and grains



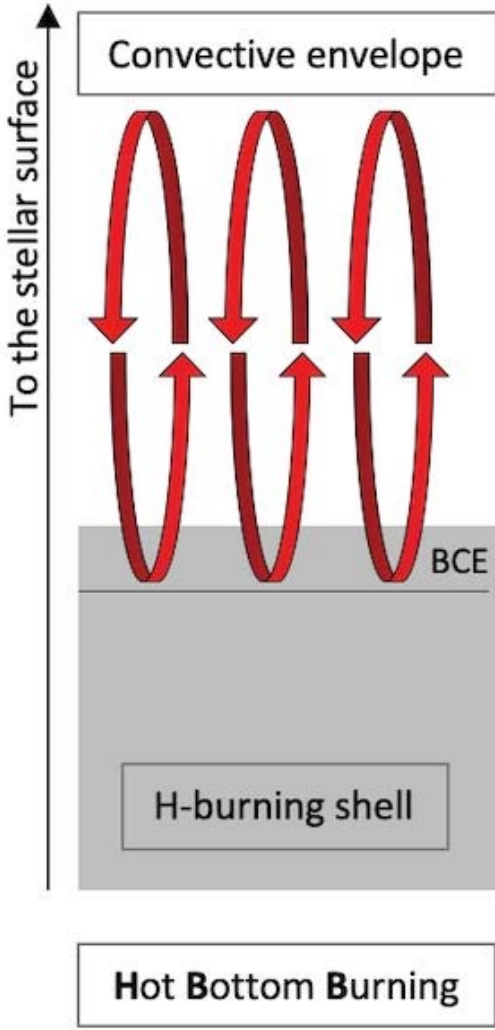
Cool Bottom Process, Bottom-up mixing or Hot Bottom Burning



Low mass AGB stars

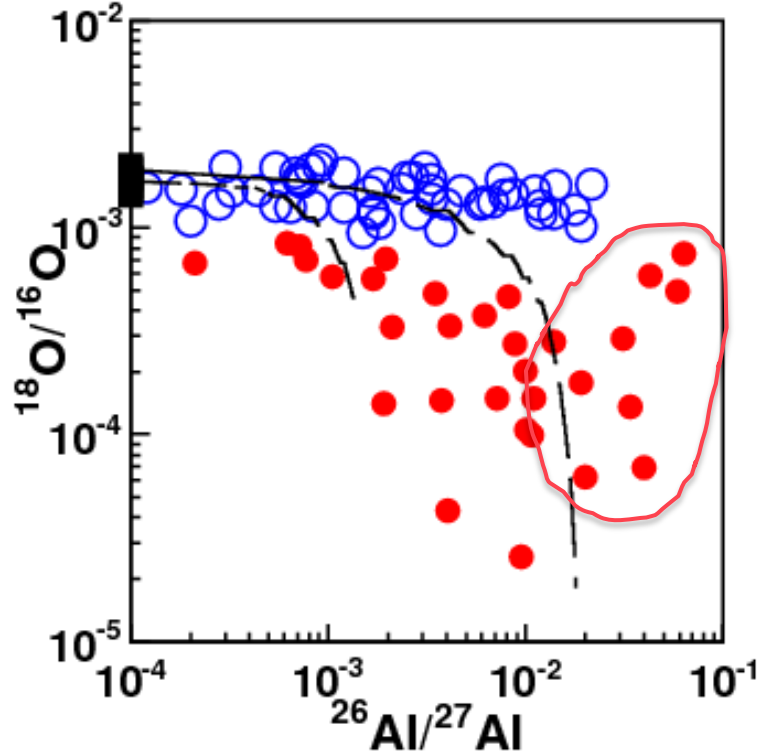


Low mass AGB stars



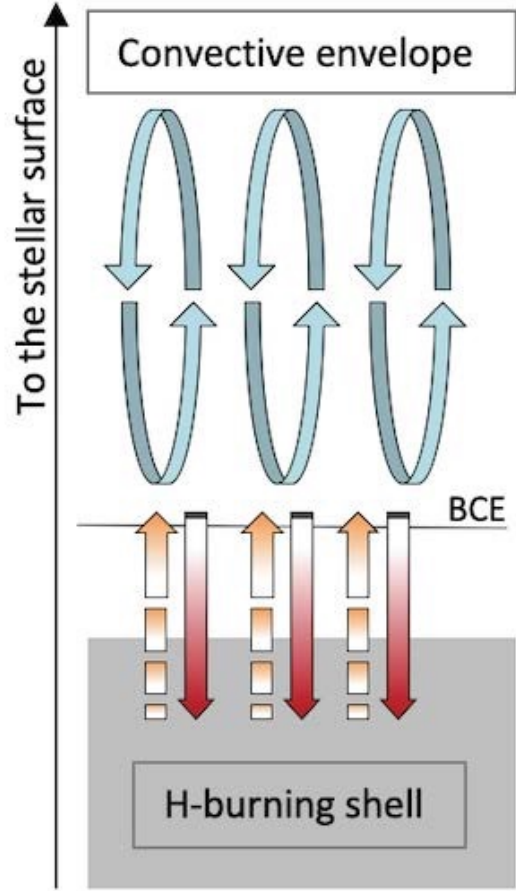
Intermediate mass AGB stars

Cool Bottom Process, Bottom-up mixing or Hot Bottom Burning



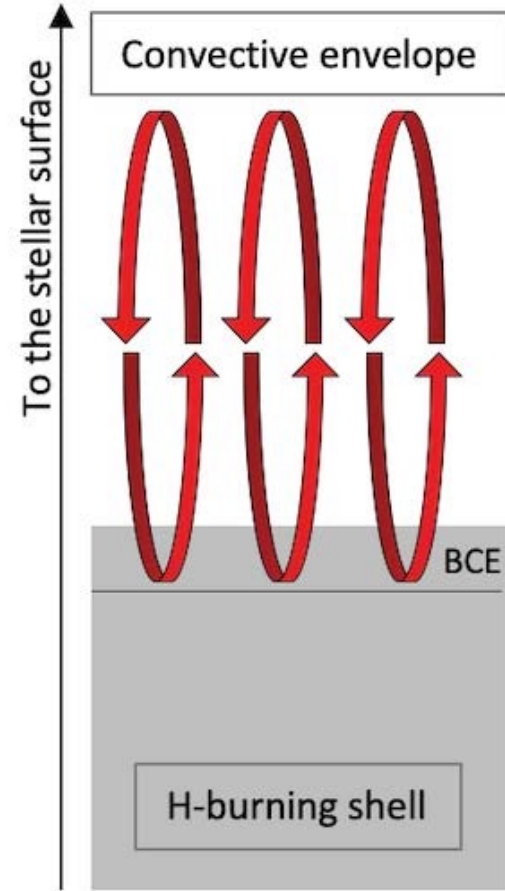
Cool Bottom Process

Low mass AGB stars



MHD extra-mixing

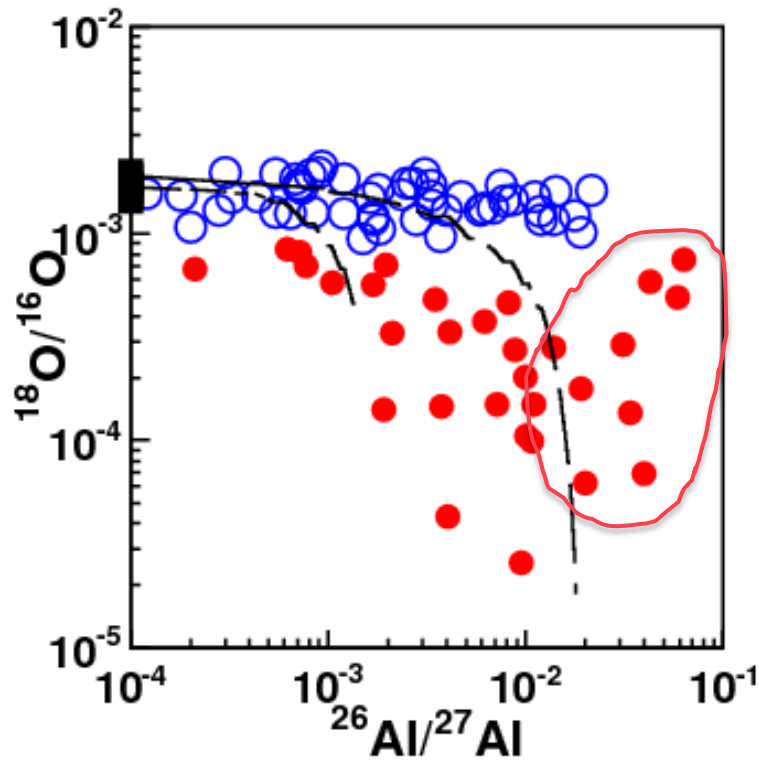
Low mass AGB stars



Hot Bottom Burning

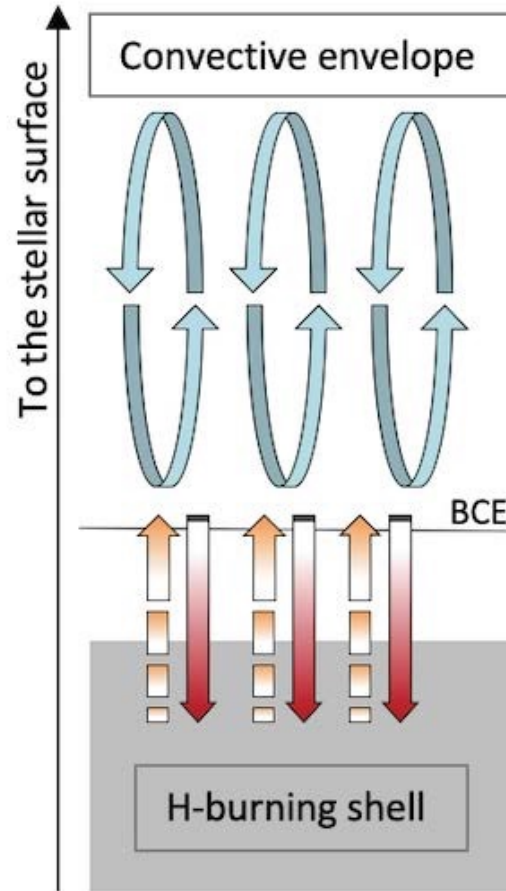
Intermediate mass AGB stars

Cool Bottom Process, Bottom-up mixing or Hot Bottom Burning



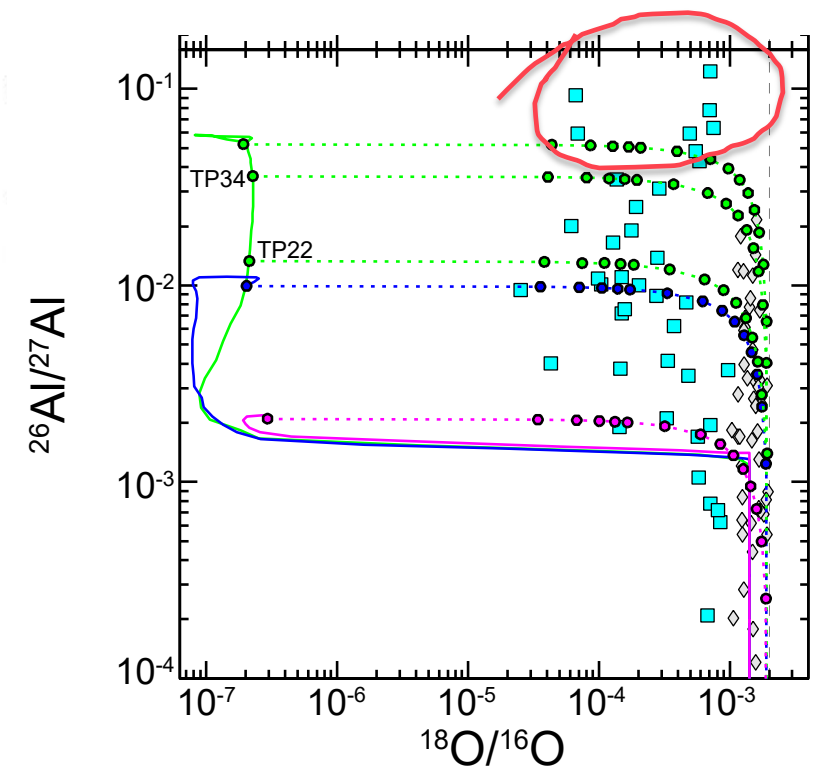
Cool Bottom Process

Low mass AGB stars



MHD extra-mixing

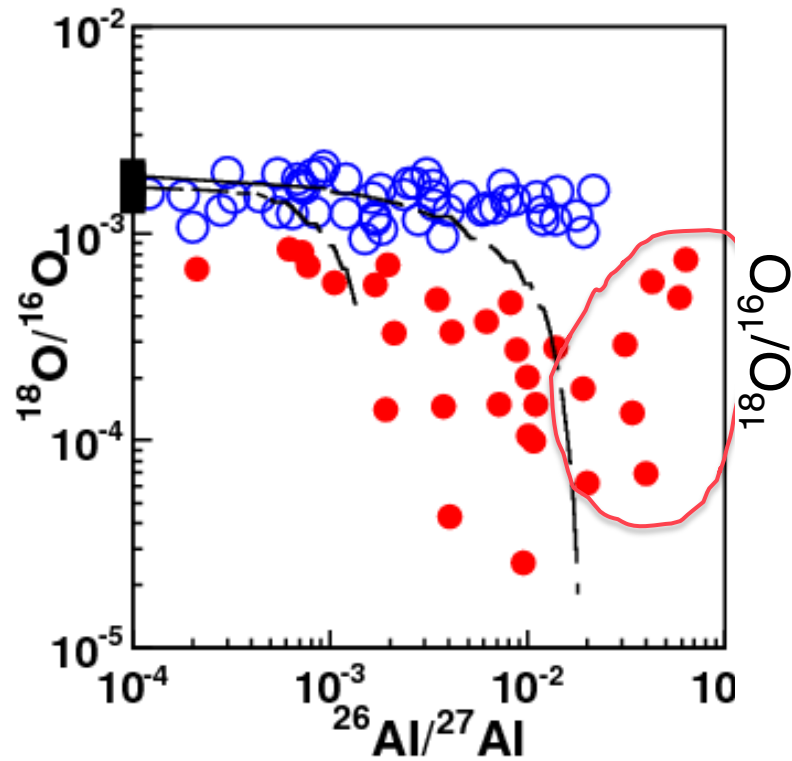
Low mass AGB stars



Hot Bottom Burning

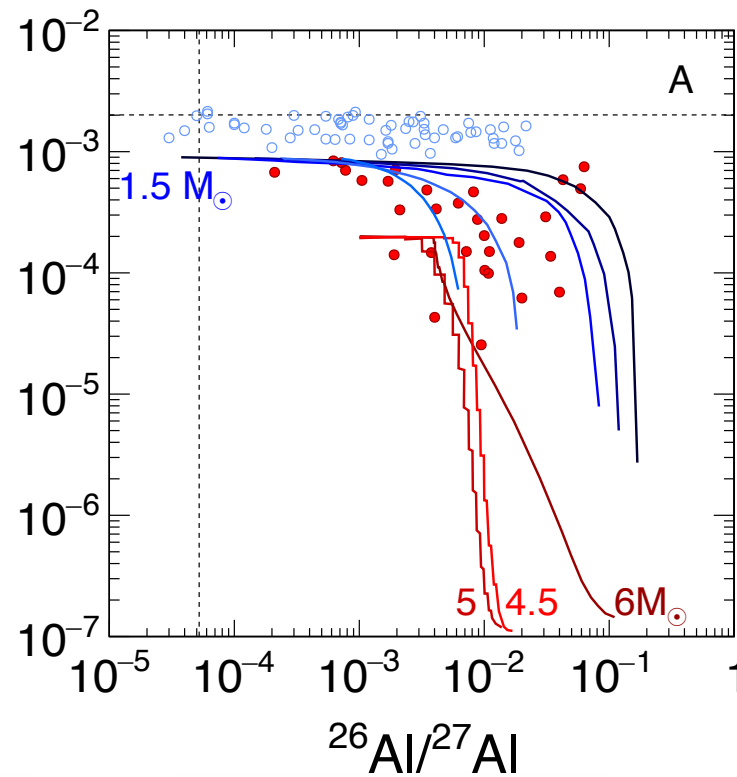
Intermediate mass AGB stars

Cool Bottom Process, Bottom-up mixing or Hot Bottom Burning



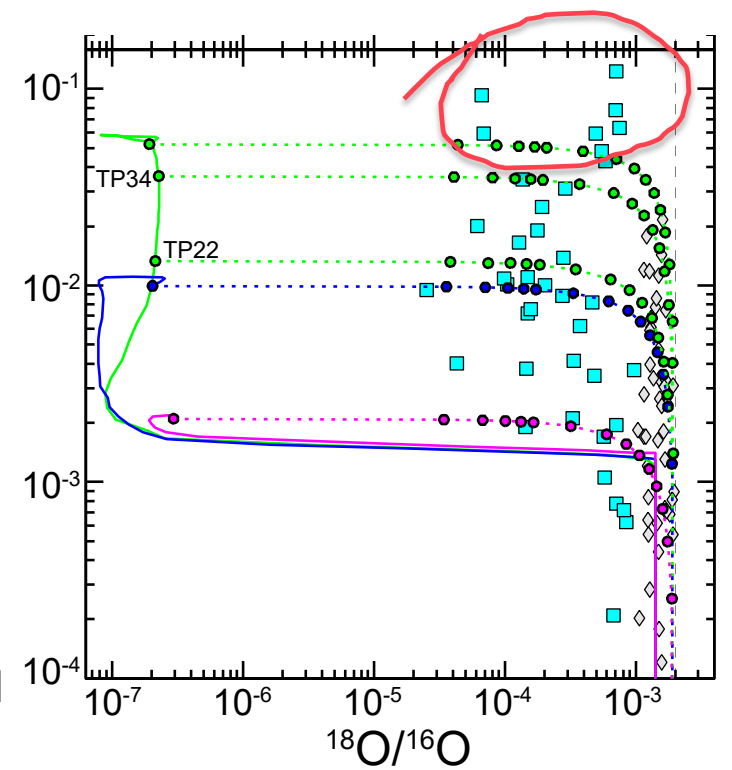
Cool Bottom Process

Low mass AGB stars



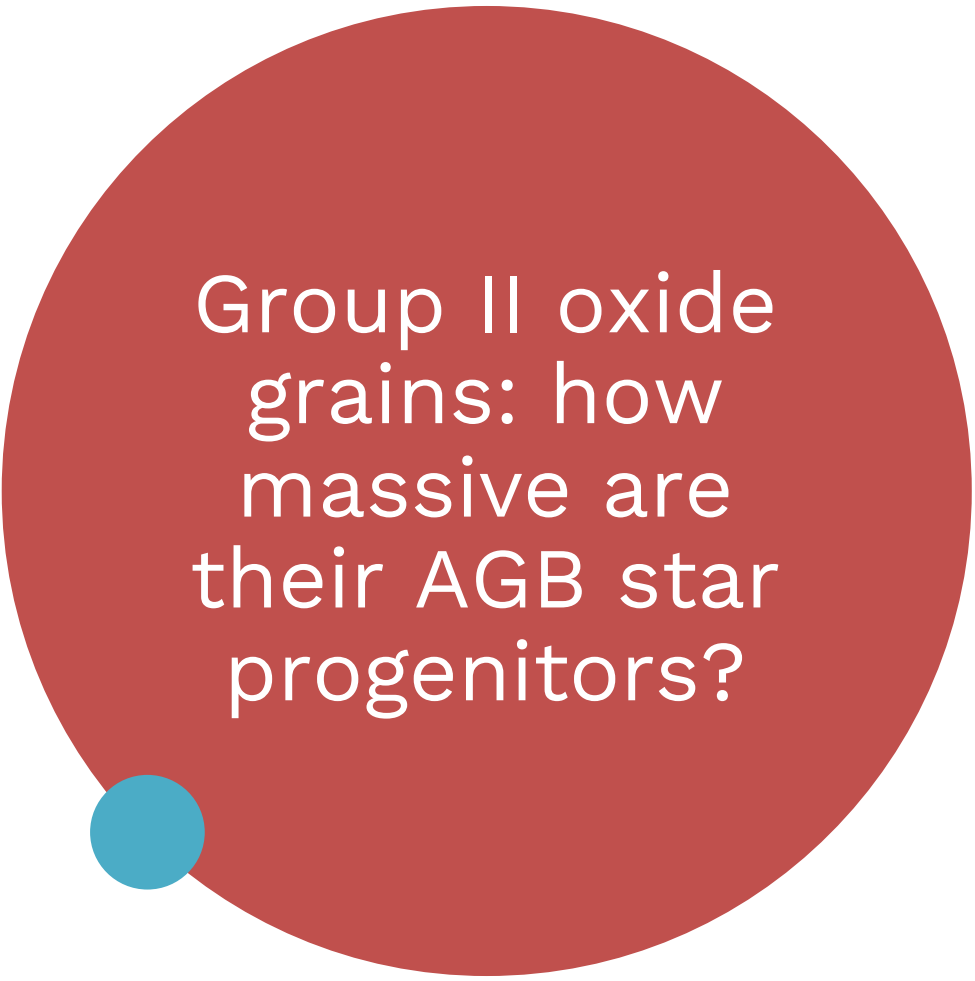
MHD extra-mixing

Low mass AGB stars

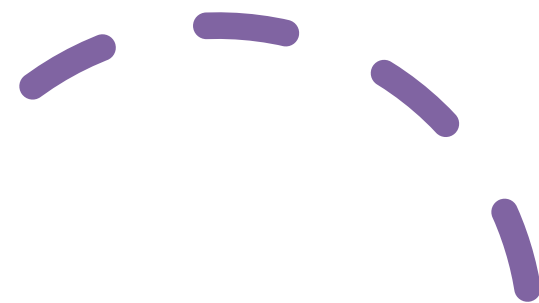


Hot Bottom Burning

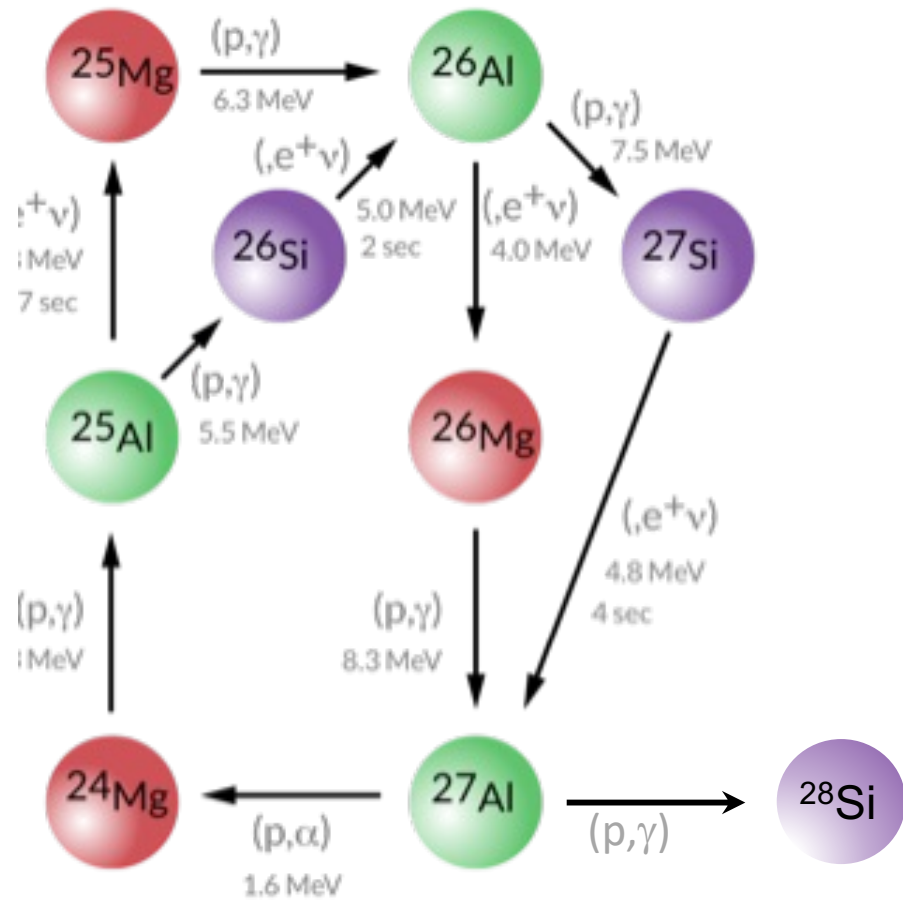
Intermediate mass AGB stars



Group II oxide grains: how massive are their AGB star progenitors?



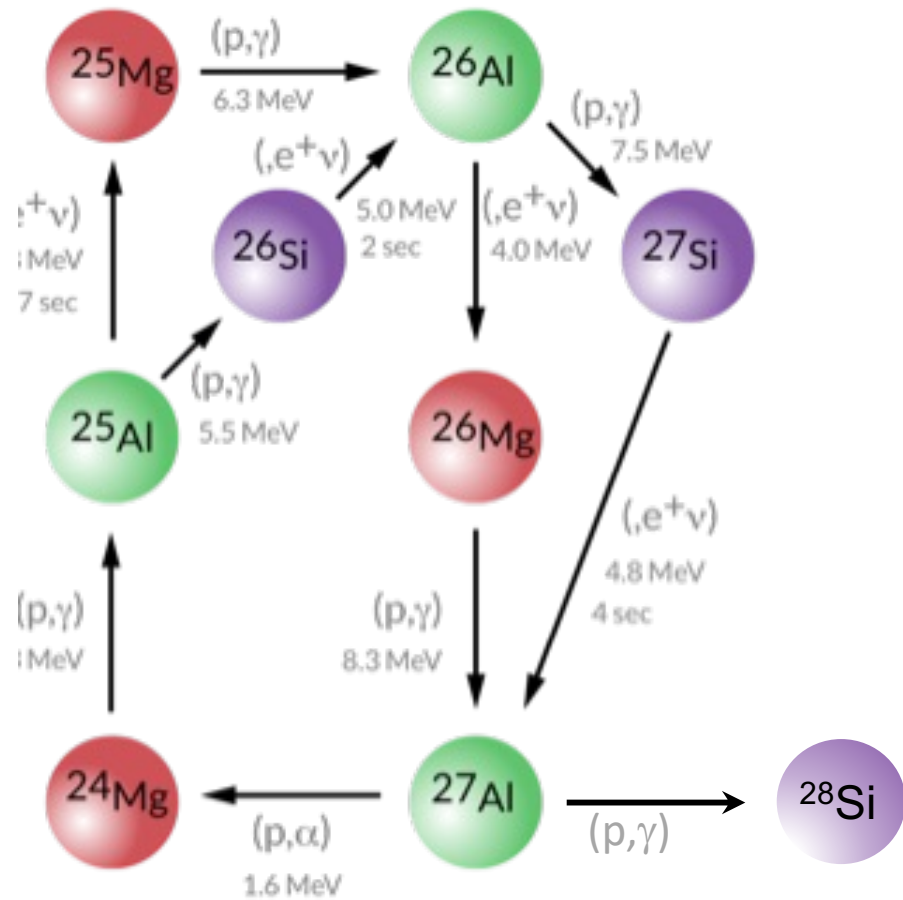
Could their $^{26}\text{Al}/^{27}\text{Al}$ relative abundances give the answer?



Mg-Al Cycles

^{26}Al in group 2 oxide grains

- A bottom-up mixing mechanism means carrying into the envelope materials from deeper/hotter stellar layers
- The same effects may come with a more efficient rate of the $^{25}\text{Mg}(p,\gamma)^{26}\text{Al}$ or a less efficient one for the $^{26}\text{Al} + p$ reactions
- In the shown calculations:
 - $^{25}\text{Mg}(p,\gamma)^{26}\text{Al}$ -> Straniero et al. 2013
 - $^{26}\text{Al}(p,\gamma)^{26}\text{Al}$ -> Iliadis et al. 2010



Mg-Al Cycles

^{26}Al in group 2 oxide grains

- A bottom-up mixing mechanism means carrying into the envelope materials from deeper/hotter stellar layers
- The same effects may come with a more efficient rate of the $^{25}\text{Mg}(p,\gamma)^{26}\text{Al}$ or a less efficient one for the $^{26}\text{Al} + p$ reactions
- In the shown calculations:
 - $^{25}\text{Mg}(p,\gamma)^{26}\text{Al}$ -> Straniero et al. 2013
 - $^{26}\text{Al}(p,\gamma)^{26}\text{Al}$ -> Iliadis et al. 2010

sensitivity studies show that uncertainty of $^{26}\text{Al} + p$ leads to variations of up to 2 orders of magnitude in AGB calculations but...

$^{26}\text{Al}^g(p,\gamma)^{27}\text{Si}$ @ H-burning T

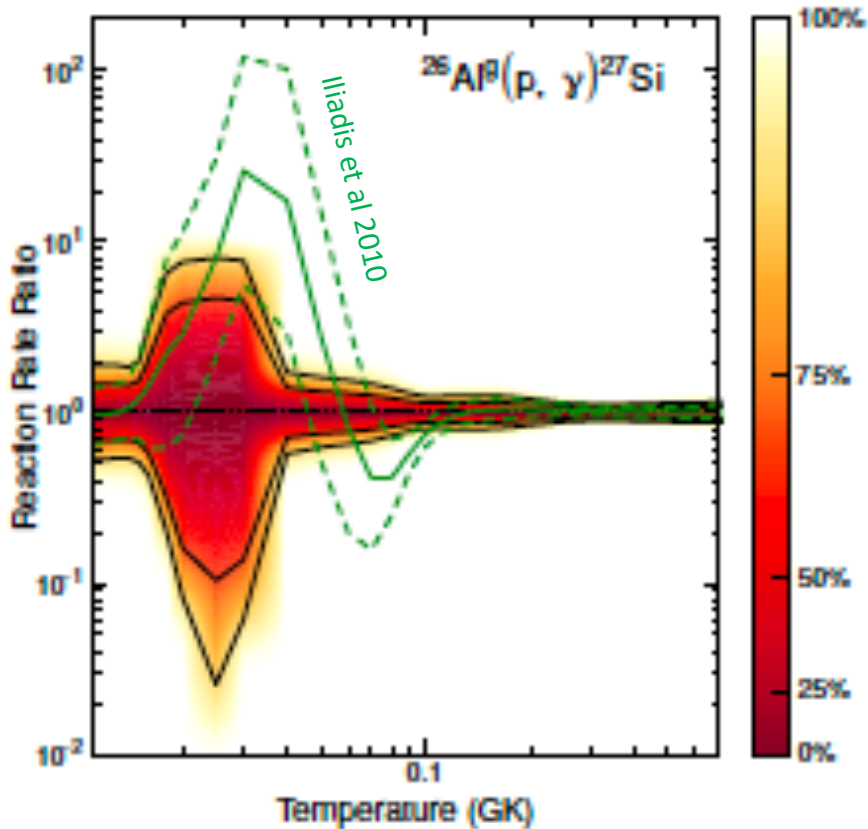


Table 2. Recommended excitation energies (E_x) together with the spins and parities (J^π) (taken from Ref. [222]) for the excited states above the proton separation energy ($S_p = 7463.34(13)$) keV [181]) in ^{27}Si for the $^{26}\text{Al}^g(p,\gamma)^{27}\text{Si}$ reaction. The resonance energies (E_{res}) and experimentally determined resonance strengths ($\omega\gamma$) for the relevant states are given where available. The atomic shift for this reaction is $\Delta B_e = 1.29$ keV. Only states producing resonances below $E_{res} = 300$ keV have been listed.

E_x (keV)	J^π	E_{res} (keV)	$\omega\gamma$ (eV)
7468.8(8)	$(1/2, 5/2)^+$	6.7(8)	$< 1.8 \times 10^{-63}$ [212]
(7493.1(40))	$(3/2^+)$	(31(4))	$< 1.5 \times 10^{-28}$ *
7531.3(7)	$5/2^+$	69.2(7)	$< 3.0 \times 10^{-15}$ [103]
(7557(3)) [212]	$(3/2^+)$	(95(3))	$< 8.0 \times 10^{-16}$ [215]
			$< 3.4 \times 10^{-15}$ [103]
			$< 5.9 \times 10^{-6}$ [213]
→ 7590.1(9)	$9/2^+$	128.0(9)	$2.6_{-0.9}^{+0.7} \times 10^{-8}$ [103]
			$2.5(5) \times 10^{-8}$ [215]
7651.9(6)	$11/2^+$	189.8(6)	$35(7) \times 10^{-6}$ [207]
7693.8(9)	$5/2^+$	231.7(9)	$< 1.0 \times 10^{-5}$ [208]
7704.3(2)	$7/2^+$	242.2(2)	$1.0(5) \times 10^{-5}$ [208]
7739.3(4)	$9/2^+$	277.2(4)	$3.8(10) \times 10^{-3}$ [227]

Laird A. et al 2022 Journal of Physics G
 Progress on nuclear reaction rates affecting
 the stellar production of ^{26}Al

$^{26}\text{Al}^g(p,\gamma)^{27}\text{Si}$ @ H-burning T

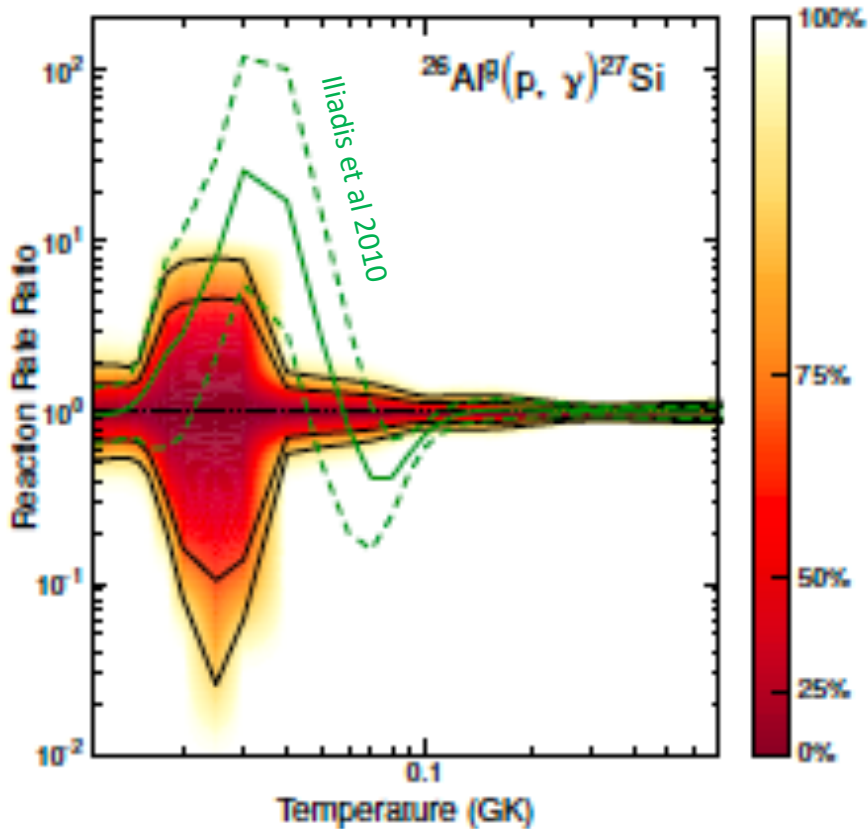


Table 2. Recommended excitation energies (E_x) together with the spins and parities (J^π) (taken from Ref. [222]) for the excited states above the proton separation energy ($S_p = 7463.34(13)$) keV [181]) in ^{27}Si for the $^{26}\text{Al}^g(p,\gamma)^{27}\text{Si}$ reaction. The resonance energies (E_{res}) and experimentally determined resonance strengths ($\omega\gamma$) for the relevant states are given where available. The atomic shift for this reaction is $\Delta B_e = 1.29$ keV. Only states producing resonances below $E_{res} = 300$ keV have been listed.

E_x (keV)	J^π	E_{res} (keV)	$\omega\gamma$ (eV)
7468.8(8)	(1/2, 1/2) ⁺	6.7(8)	$< 1.5 \times 10^{-63}$ [212]
(7493.1(40))	(3/2, 1/2) ⁺	(31(4))	$< 5 \times 10^{-28}$ *
7531.3(7)	5/2 ⁺	69.2(7)	$< 3.5 \times 10^{-15}$ [103]
(7557(3)) [212]	(3/2 ⁺)	(95(3))	$< 9 \times 10^{-16}$ [215]
			$< 1 \times 10^{-15}$ [103]
			$< 5 \times 10^{-6}$ [213]
→ 7590.1(9)	9/2 ⁺	128.0(9)	$2.6_{-0.2}^{+0.3} \times 10^{-8}$ [103]
			$2.5(5) \times 10^{-15}$ [15]
7651.9(6)	11/2 ⁺	189.8(6)	$35(7) \times 10^{-8}$ [207]
7693.8(9)	5/2 ⁺	231.7(9)	$< 1.0 \times 10^{-5}$ [208]
7704.3(2)	7/2 ⁺	242.2(2)	$1.0(5) \times 10^{-5}$ [208]
7739.3(4)	9/2 ⁺	277.2(4)	$3.8(10) \times 10^{-3}$ [227]

Laird A. et al 2022 Journal of Physics G
 Progress on nuclear reaction rates affecting
 the stellar production of ^{26}Al

The 228keV isomeric state must be treated separately from the ground state at temperatures below 0.4 GK

$^{26}\text{Al}^m(p,\gamma)^{27}\text{Si}$ @ H-burning T

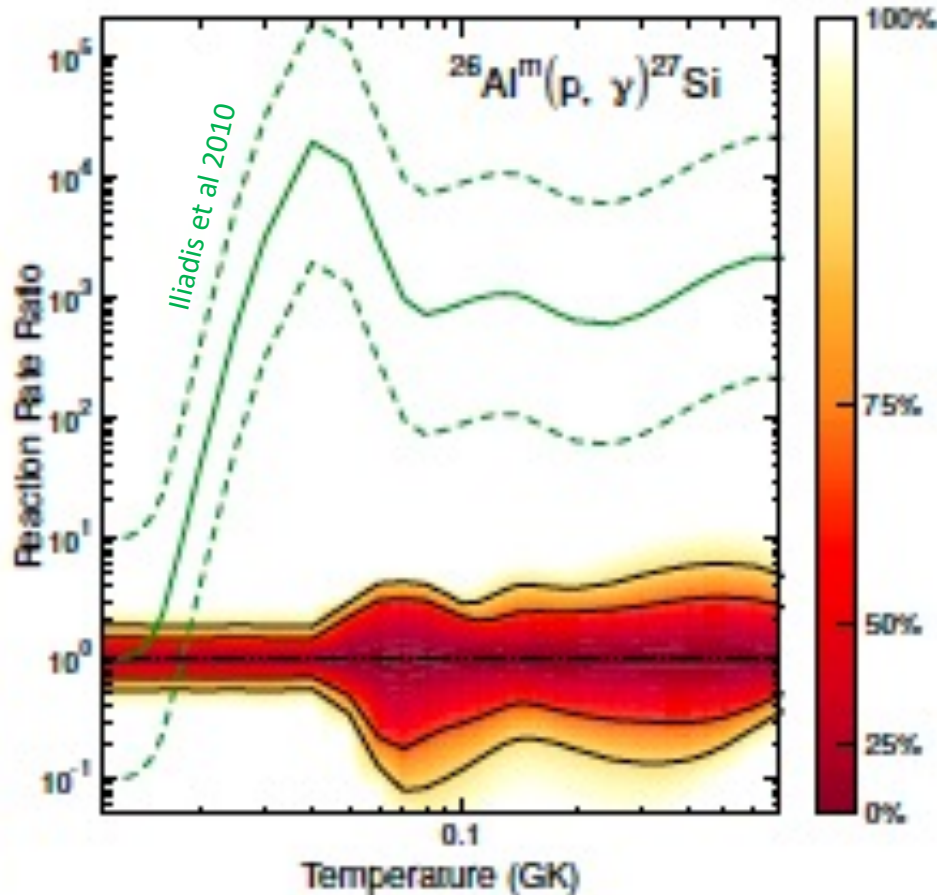


Table 3. Recommended excitation energies (E_x) together with the spins and parities (J^π) (taken from Ref. [222]) for the excited states above the proton separation energy ($S_p = 7691.65(13)$ keV [181]) in ^{27}Si for the $^{26}\text{Al}^m(p,\gamma)^{27}\text{Si}$ reaction. The resonance energies (E_{res}) and experimentally determined resonance strengths ($\omega\gamma$) for the relevant states are given where available. The atomic shift for this reaction is $\Delta B_e = 1.29$ keV. Only states producing resonances below $E_{res} = 400$ keV have been listed.

E_x (keV)	J^π	E_{res} (keV)	$\omega\gamma$ (eV)
7693.8(9)	5/2 ⁺	3.5(9)	$< 2.90 \times 10^{-86}$
7704.3(2)	7/2 ⁺	14.0(2)	$< 4.61 \times 10^{-44}$
7739.3(4)	9/2 ⁺	49.0(4)	$< 2.69 \times 10^{-22}$
7794.8(19)	7/2 ⁺	104.5(19)	$< 1.92 \times 10^{-14}$
7831.5(5)	9/2 ⁻	141.2(5)	$< 2.39 \times 10^{-14}$
7837.6(2)	5/2 ⁺	147.2(2)	$< 1.47 \times 10^{-8}$ [228]
7899.0(8)	5/2 ⁺	208.7(8)	$< 1.61 \times 10^{-5}$
7909.1(7)	3/2 ⁺	218.8(7)	$< 1.42 \times 10^{-6}$ [228]
7966.3(8)	5/2 ⁺	276.0(8)	$< 2.40 \times 10^{-2}$
8031.5(11)	5/2 ⁺	341.2(11)	$< 3 \times 10^{-8}$ [226]
8069.6(30)	3/2 ⁻	379.3(30)	$< 3.20 \times 10^{-4}$ [226]

The 228keV isomeric state must be treated separately from the ground state at temperatures below 0.4 GK

$^{26}\text{Al}^m(p,\gamma)^{27}\text{Si}$ @ H-burning T

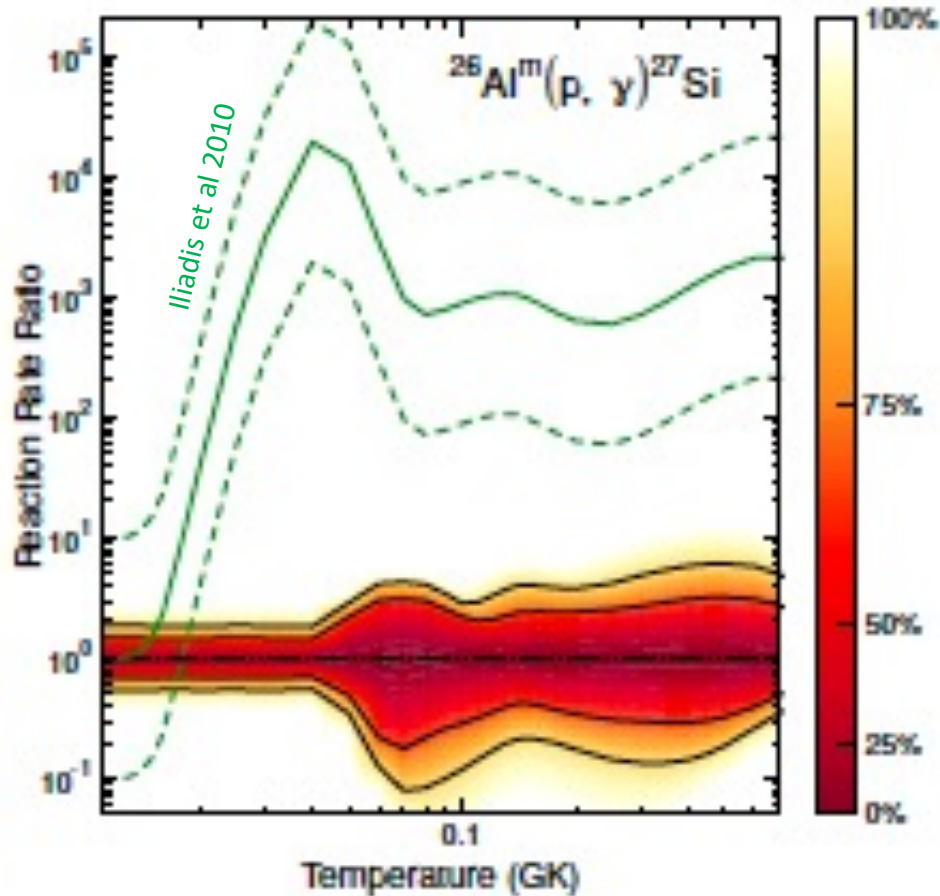
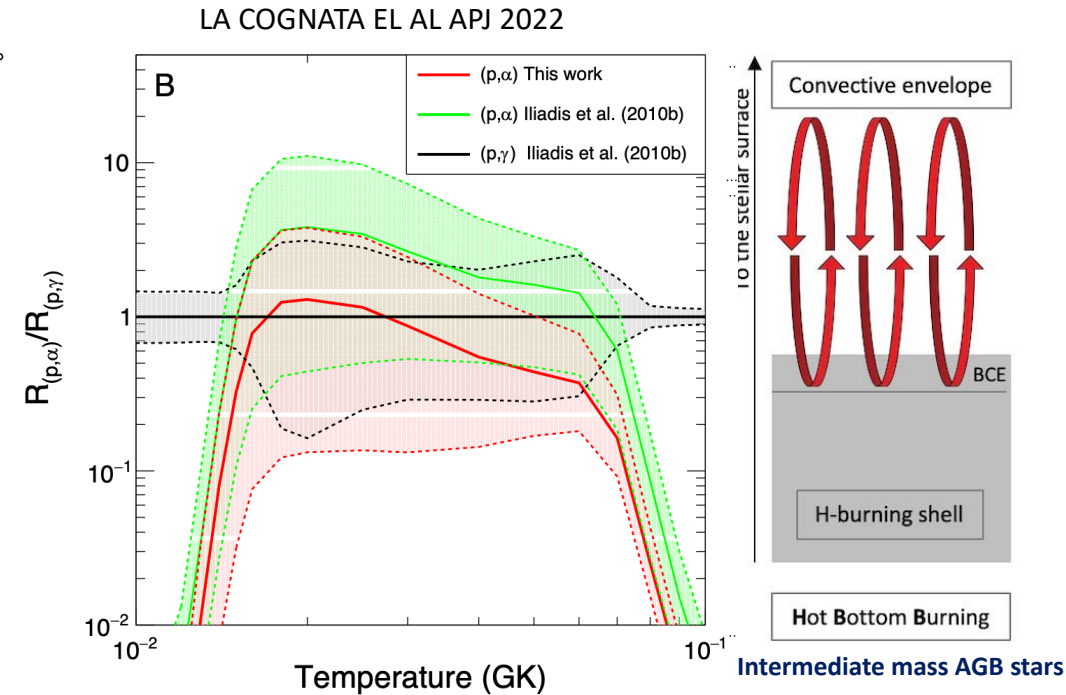
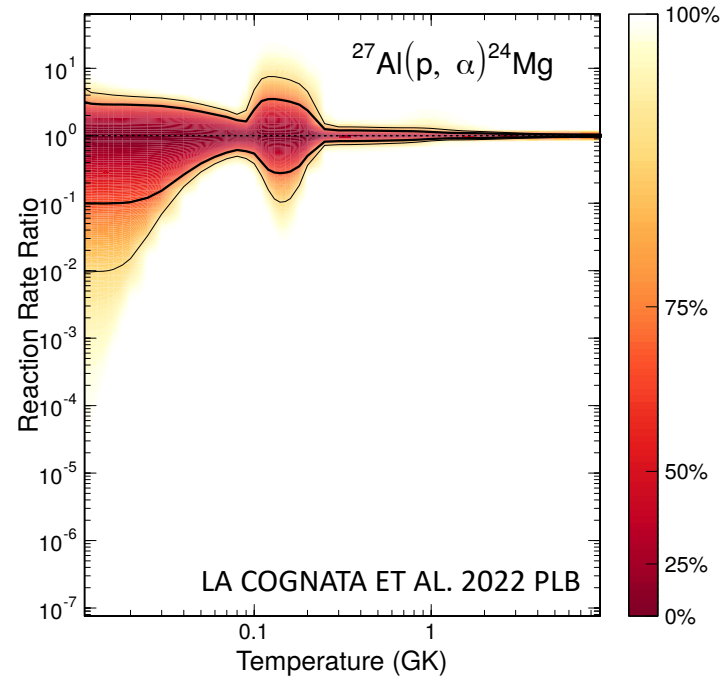


Table 3. Recommended excitation energies (E_x) together with the spins and parities (J^π) (taken from Ref. [222]) for the excited states above the proton separation energy ($S_p = 7691.65(13)$ keV [181]) in ^{27}Si for the $^{26}\text{Al}^m(p,\gamma)^{27}\text{Si}$ reaction. The resonance energies (E_{res}) and experimentally determined resonance strengths ($\omega\gamma$) for the relevant states are given where available. The atomic shift for this reaction is $\Delta B_e = 1.29$ keV. Only states producing resonances below $E_{res} = 400$ keV have been listed.

E_x (keV)	J^π	E_{res} (keV)	$\omega\gamma$ (eV)
7693.8(9)	5/2 ⁺	3.5(9)	$< 2.90 \times 10^{-86}$
7704.3(2)	7/2 ⁺	14.0(2)	4.61×10^{-44}
7739.3(4)	2 ⁺	49.0(4)	2.69×10^{-22}
7794.8(19)	2 ⁺	104.5(19)	1.92×10^{-14}
7831.5(5)	2 ⁻	141.2(5)	2.39×10^{-14}
7837.6(2)	5/2 ⁻	147.2(2)	1.47×10^{-8} [228]
7899.0(8)	5/2 ⁺	177.0(8)	1.1×10^{-5}
7909.1(7)	3/2 ⁺	218.8(7)	$< 1.1 \times 10^{-6}$ [228]
7966.3(8)	5/2 ⁺	276.0(8)	$< 2.1 \times 10^{-2}$
8031.5(11)	5/2 ⁺	341.2(11)	$< 3 \times 10^{-8}$ [226]
8069.6(30)	3/2 ⁻	379.3(30)	$< 3.20 \times 10^{-4}$ [226]

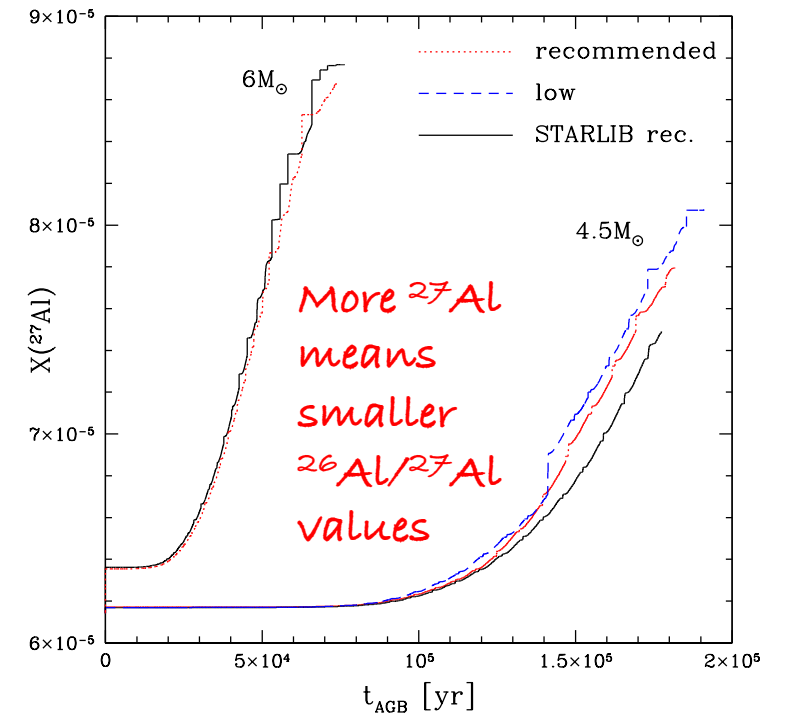
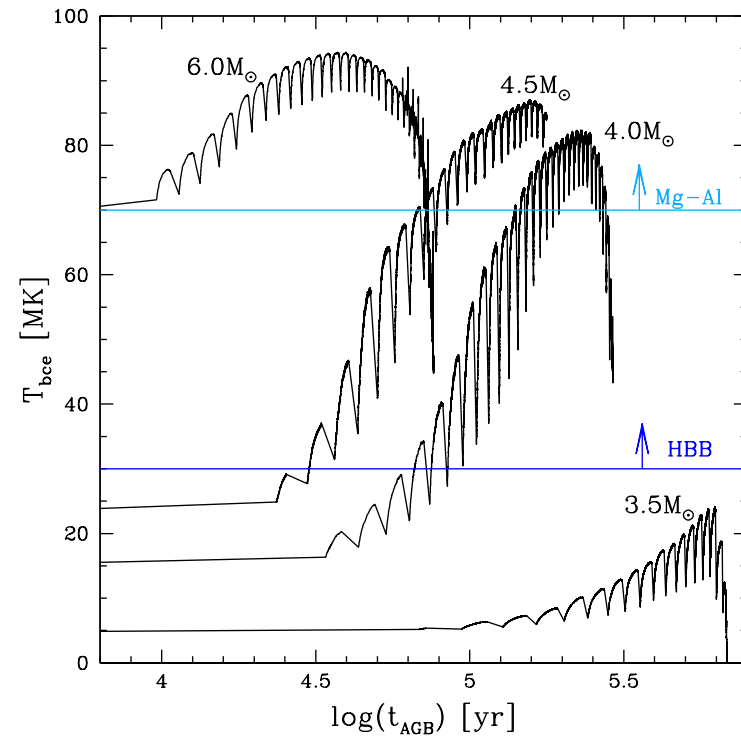
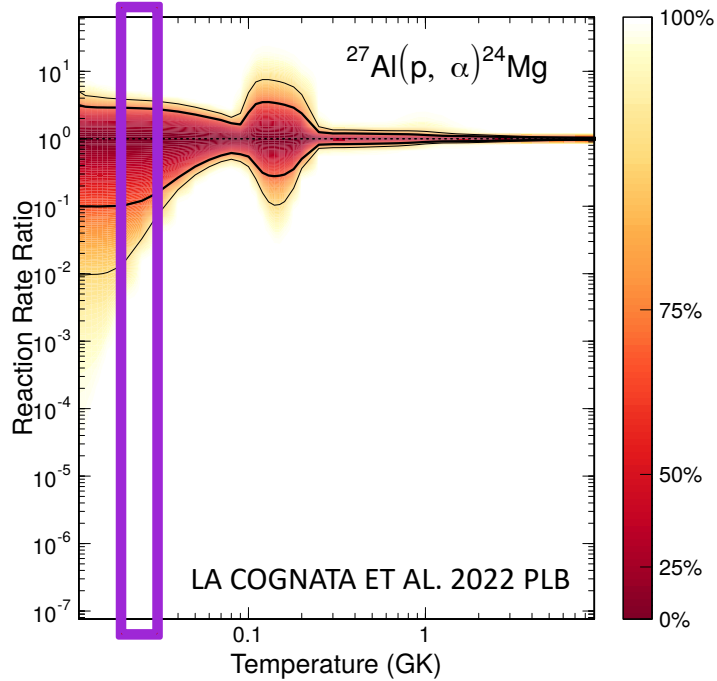
The $^{27}\text{Al}(p,\alpha)^{24}\text{Mg}$ reaction rate from a thm experiment

Energy in cm (keV)	Jpi	Strength (eV) [STARLIB]	error (eV)	Strength (eV) [THM]	error (eV)
71.5	2+	2.47E-14	up lim	9.28E-15	up lim
84.3	1-	2.60E-13	up lim	1.90E-14	4.7E-15
193.5	2+	3.74E-07	up lim	2.82E-07	up lim
214.7	3-	1.13E-07	up lim	4.92E-08	up lim
486.74	2+	0.11	0.05	0.122	0.031
609.49	3-	0.275	0.069	0.282	0.082
705.08	1-	0.52	0.13	0.30	0.10
855.85	3-	0.83	0.21	0.71	0.56
903.54	3-	4.3	0.4	4.3	0.4
1140.88	2+	79	27	83	21
1316.7	2+	137	47	142	43
1388.8	1-	54	15	70	18



- The reaction rate is about 3 times lower than presently assumed, at H-burning T
- in LMS the rate effect is not appreciable because the (p,γ) channel strongly dominates

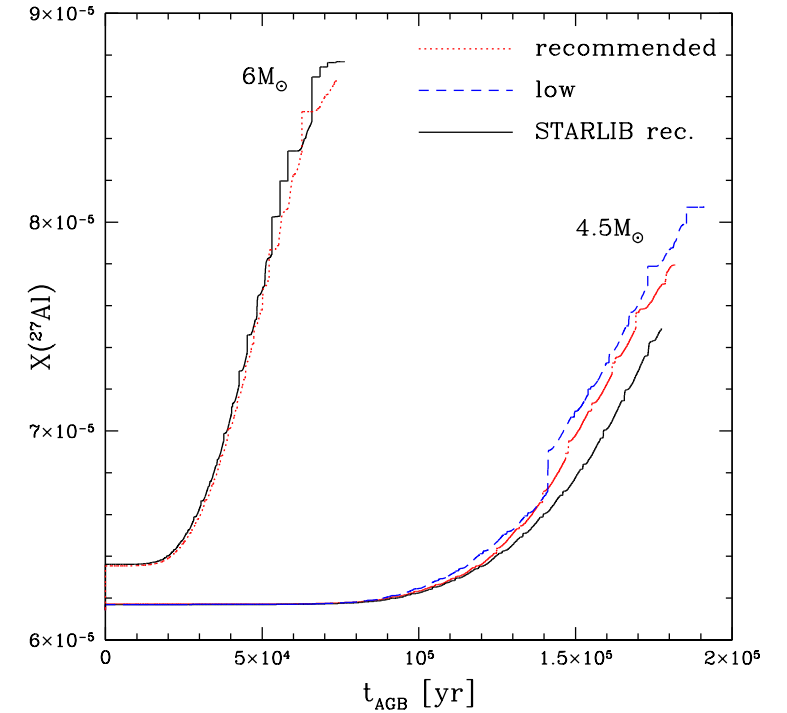
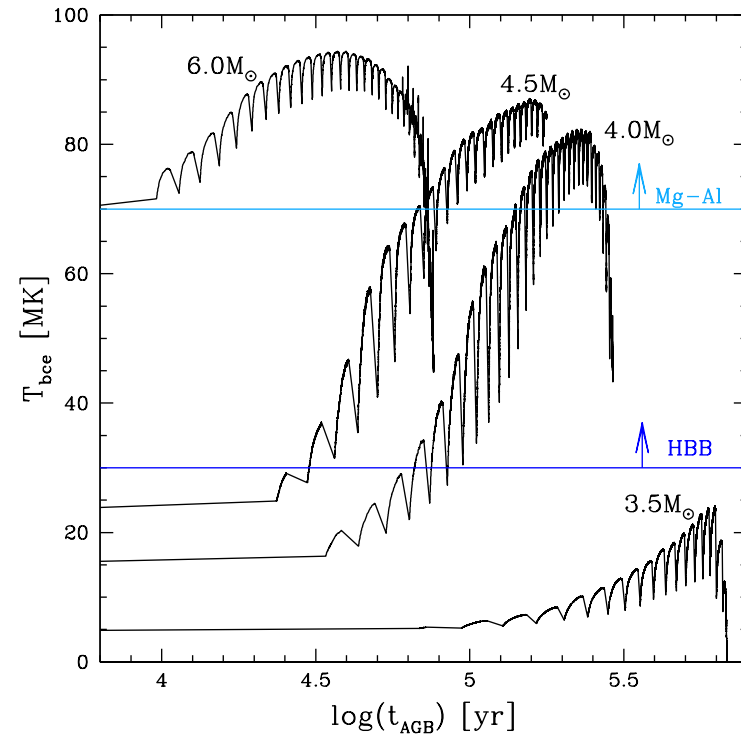
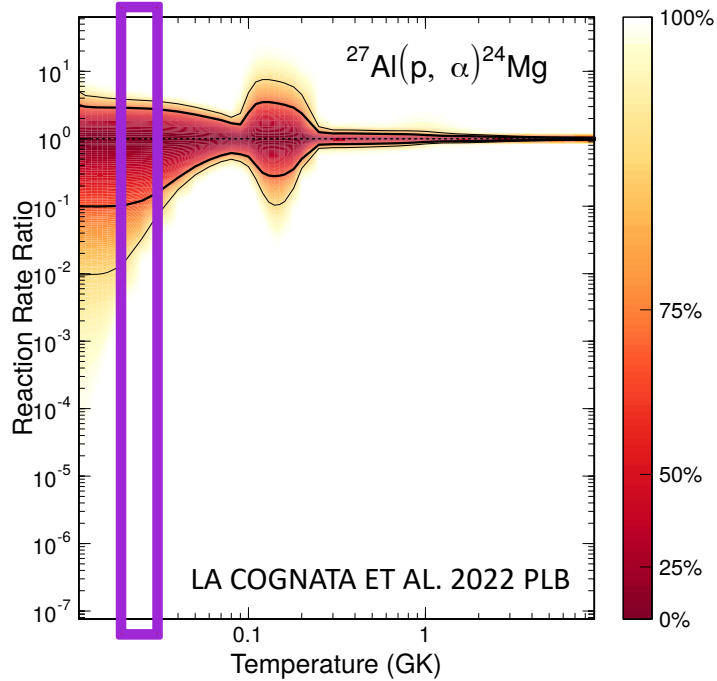
The $^{27}\text{Al}(p,\alpha)^{24}\text{Mg}$ Implications for Nucleosynthesis



LA COGNATA ET AL APJ 2022

Evolution of the temperature at the base of the convective envelope as function of the time counted from the beginning of the AGB phase. Stars with 3.5, 4.0, 4.5 and 6.0 M_{\odot} initial masses and Z_{\odot}

The $^{27}\text{Al}(p,\alpha)^{24}\text{Mg}$ Implications for Nucleosynthesis



Evolution of the temperature at the base of the convective envelope as function of the time counted from the beginning of the AGB phase. Stars with 3.5, 4.0, 4.5 and 6.0 M_{\odot} initial masses and Z_{\odot} .

Conclusions:



- ★ LM AGB stars + bottom-up deep mixing can be progenitors of group 2 oxide grains
 - the agreement between models and observations becomes better or worse according with the nuclear physics input,
 - In any case models provides a match to the majority of the grains.

- ★ IM AGB stars + HBB can also be progenitors of group 2 oxide grains
 - the agreement i between models and grains are good just using the more efficient $^{17}\text{O}+p$ reaction rates
 - Dilution effects have to be included to provides a match to the majority of the grains.

- ★ At the moment LM AGB models with a bottom-up advective mixing at play provide the most accurate fits to group 2 oxide grain composition, well reproducing $^{26}\text{Al}/^{27}\text{Al}$ of the majority of the grains.

- ★ the abundances of ^{17}O and ^{26}Al are thermometers of their nucleosynthesis environments:
 - to well calibrate them and make them accurate we need very precise knowledge of the reactions that produce and destroy them.
 - $^{26}\text{Al} + p$ and its decay in particular

Conclusions:



Many
thanks!!!

- ★ LM AGB stars + bottom-up deep mixing can be progenitors of group 2 oxide grains
 - the agreement between models and observations becomes better or worse according with the nuclear physics input,
 - In any case models provides a match to the majority of the grains.
- ★ IM AGB stars + HBB can also be progenitors of group 2 oxide grains
 - the agreement i between models and grains are good just using the more efficient $^{17}\text{O}+p$ reaction rates
 - Dilution effects have to be included to provides a match to the majority of the grains.
- ★ At the moment LM AGB models with a bottom-up advective mixing at play provide the most accurate fits to group 2 oxide grain composition, well reproducing $^{26}\text{Al}/^{27}\text{Al}$ of the majority of the grains.
- ★ the abundances of ^{17}O and ^{26}Al are thermometers of their nucleosynthesis environments:
 - to well calibrate them and make them accurate we need very precise knowledge of the reactions that produce and destroy them.
 - $^{26}\text{Al} + p$ and its decay in particular